Earthline Journal of Mathematical Sciences

E-ISSN: 2581-8147

Volume 15, Number 4, 2025, Pages 649-683 https://doi.org/10.34198/ejms.15425.649683



Mathematical Analysis of a Tuberculosis-Schistosomiasis Co-infection Model with Vaccination and Treatment

I. I. Ako^{1,*} and R. U. Omoregie²

Department of Mathematics, University of Benin, Benin City, Nigeria e-mail: ignatius.ako@uniben.edu

² Department of Mathematics, University of Benin, Benin City, Nigeria e-mail: rosemary.omoregie@uniben.edu

Abstract

We present a mathematical model, that is deterministic, for investigating the impact of schistosomiasis infection on the immunogenicity of the BCG vaccine affects the use of vaccination as a measure of control against TB infection at population level in Nigeria. The presence of the backward bifurcation phenomenon was established from the analysis of the model, and it was discovered that the following parameters were responsible the adjustment parameter for comparative contagiousness of individuals re-contaminated with TB (Θ_{RT}) , the rate of therapy for schistosomiasis-only infected persons (ζ_S) , the impact of schistosomiasis on the BCG protection against TB (ζ_{TS}) , BCG vaccine waning (θ_V) , the BCG vaccine efficacy (ϵ_1) , the treatment rate for TB (ζ_T) , the comparative rates by which individuals having dormant schistosomiasis (η_1) cum virulent schistosomiasis (η_2) are tainted with TB, correspondingly, the depreciated rate of contamination with schistosomiasis (ψ), the regulation parameter for comparative infectiousness of persons possessing virulent TB cum dormant schistosomiasis (Π_1), the treatment rate for TB for co-infected persons (ζ_{T1}), the progression rate from contagious TB/unprotected from schistosomiasis to contagious TB/contagious schistosomiasis (σ) , and the rate of advancement from unprotected against the two infirmities TB/schistosomiasis to unprotected against TB/infectious schistosomiasis (α_2). The disease-free equilibrium was found to be globally asymptotically stable when the parameters responsible for the backward bifurcation phenomenon were negligible, the the effective reproduction number is less than unity.

1 Introduction

Tuberculosis (TB), generated by $Mycobacterium\ tuberculosis$, affects about a third of global population with 2 - 3 million deaths as casualties annually is of serious public health concern around the world [33, 60, 62]. TB is responsible for morbidity among several millions of people worldwide. Only a tenth

Received: February 1, 2025; Revised & Accepted: May 7, 2025; Published: May 15, 2025

2020 Mathematics Subject Classification: 93B99.

Keywords and phrases: BCG, backward bifurcation, co-infection, schistosomiasis, tuberculosis.

*Corresponding author

Copyright © 2025 the Authors

of individuals that are infected TB progress to active TB [60]. A total of 1.25 million persons suffered mortality as a result of TB in 2023 [66]. 6.4 million individuals were identified as fresh cases by the WHO in 2017 [62,63]. An estimated 10.8 million people took ill with TB globally, comprising of 6.0 million, 3.6 million women and 1.3 million [66]. TB is both curable and preventable [66]. Worldwide efforts to fight TB has saved about 79 million lives since the year 2000 [66]. In certain places, the Bacille Calmette-Guérin vaccine, popularly known as the BCG vaccine, is administered to babies or little children to prevent TB; this vaccine prevents children from serious forms of and mortality from the disease [66].

Schistosomiasis, on the other hand, ranks only behind malaria in the tropics, is regarded as an NTD, i.e., a neglected tropical disease, caused by parasitic worms (blood flukes) of the genus *Schistosoma* [12,28]. It was estimated in 2021 that a minimum of 251.4 million persons needed preventive treatment [65]; such protective therapeutic care which should be re-administered over a couple of years, has the propensity to lower and prevent morbidity [65]. About 78 countries have reported cases of schistosomiasis transmission [65].

It has already been established in the literature that TB and schistosomiasis co-infection does exist in overlapping regions where both diseases coexist [30, 50, 59].

Parasitic worm infections are common globally and can set-off effective protective reactions that are different from and in addition, possibly counteract host protective reactions to disease-inflicting microbes [53]. It is indicative that a misrepresented Th2 reaction precipitated by *S. mansoni* infection endangers safeguards activated in human beings by *M. bovis*' BCG vaccination [19,22,23,33] and in mice systemically infected with *Mtb* [21,33]. Amazingly, although parasitic worm co-infections boost *M. bovis* BCG [20,33] and *M. tuberculosis* [33,50] lung hardship, the escalation in mycobacterial load is often ephemeral [33,50] and balanced [20,33,50], implying that the consequence of parasitic worm co-infections on *Mtb* restriction is not sufficient to totally describe the heightened acerbity of TB in parasitic worm-co-infected humans detected in regions that are endemic with TB [33].

Several authors have contributed immensely to the literature as far as the mathematical modelling of TB is concerned [5,7,10,17,24,34,39–41,43–45,54,58]. In the same vein, a lot of authors have also enriched the literature concerning mathematical modelling of schistosomiasis via various assumptions [1,2,6,11,13–15,18,25–27,31,32,35,36,38,46–48,51,52,67–69]. It is worthy of note that it was Ako and Olowu [3] that considered the mathematical analysis of TB-schistosomisis co-infection in their novel work. However, they did not consider the impact of schistosomiasis infection on the immumogenicity of the BCG vaccine affects the use of vaccination as a control measure against TB infection at population level. This is the knowledge gap that we seek to fill through this study.

This study is categorized as follows: Section 2 contains the model formulation, Section 3 reveals the mathematical analysis of the basic properties of the model. Section 3 addresses the local asymptotic

stability of the disease-free equilibrium with a special focus on the investigation of the model for the backward bifurcation phenomenon, a special case of the global asymptotic stability of the infection-free equilibrium, and the numerical simulation of the model while fluctuating the values of some essential parameters while Section 4 concludes the study.

2 Formulation of the Model with Vaccination

The basic model in [3], is now elongated to integrate imperfect TB (BCG) vaccine. In order to achieve this, the ensuing unique variables are introduced for the population of individuals vaccinated with BCG ($V_T(t)$) and humans vaccinated with BCG and exposed to schistosomiasis ($V_{TS}(t)$). The other variables in Equation (2.1) of [3] (i.e., vulnerable to contagions ($S_H(t)$), having dormant TB but not contagious ($E_{HT}(t)$), infectious TB ($I_{HT}(t)$), externally re-contaminated with TB ($I_{RT}(t)$), cured of TB ($I_{HT}(t)$), unprotected against schistosomiasis ($E_{HS}(t)$), tainted with schistosomiasis ($I_{HS}(t)$), undergoing therapy for schistosomiasis ($I_{HS}(t)$), unprotected against TB, unprotected against schistosomiasis ($E_{TS}(t)$), having virulent TB, unprotected against schistosomiasis ($I_{RS1}(t)$), unprotected against TB, with contagious schistosomiasis ($E_{ST}(t)$), externally re-tainted with TB cum contagious schistosomiasis (I_{RS2}), and having infectious TB, infectious schistosomiasis ($I_{TS}(t)$) humans remain the same, such that the total human population is represented by

$$N_{H}(t) = S_{H}(t) + V_{T}(t) + V_{TS}(t) + E_{HT}(t) + I_{HT}(t) + I_{RT}(t) + T_{HT}(t) + E_{HS}(t) + I_{HS}(t) + T_{HS}(t) + E_{TS}(t) + I_{ST}(t) + I_{RS1}(t) + E_{ST}(t) + I_{RS2}(t) + I_{TS}(t).$$

$$(2.1)$$

Afterwards, we integrate the go-between hosts, snails of freshwater origin, for the parasite liable for schistosomiasis in the model formulation.

It is assumed, herein, that the whole population of snails domiciled in freshwater at time t, denoted by $N_S(t)$, is separated into the commonly exclusive categories of snails susceptible $(S_S(t))$ cum snails pierced with miracidia $(I_S(t))$, that is

$$N_S(t) = S_S(t) + I_S(t). (2.2)$$

As a result of the suppositions made above, the formulated model that is vaccination-based is shown in (2.3). The explanations of the classes or sub-populations and parameters deployed in the mathematical

formulation are tabulated in Tables 1, 2 and 3, respectively.

$$S'_{H} = \omega \Lambda_{H} + \theta_{V}V_{T} - \lambda_{T}S_{H} - \lambda_{J}S_{H} - \mu_{H}S_{H},$$

$$V'_{T} = (1 - \omega)\Lambda_{H} - \lambda_{J}V_{T} - (1 - \epsilon_{1})\lambda_{T}V_{T} - (\theta_{V} + \mu_{H})V_{T},$$

$$V'_{TS} = \lambda_{J}V_{T} - \zeta_{TS}\lambda_{T}V_{TS} - \mu_{H}V_{TS},$$

$$E'_{HT} = (1 - p)\lambda_{T}(S_{H} + \xi T_{HT} + T_{HS}) + (1 - \epsilon_{1})\lambda_{T}V_{T} + \zeta_{S1}E_{ST}$$

$$- (1 - \pi_{1})\lambda_{T}E_{HT} - \lambda_{J}E_{HT} - (\kappa_{1} + \mu_{H})E_{HT},$$

$$I'_{HT} = p\lambda_{T}(S_{H} + \xi T_{HT} + T_{HS}) + \kappa_{1}E_{HT} + \zeta_{S3}I_{TS} - \lambda_{J}I_{HT}$$

$$- (\zeta_{T} + \delta_{T} + \mu_{H})I_{HT},$$

$$I'_{RT} = (1 - \pi_{1})\lambda_{T}E_{HT} + \zeta_{S2}I_{RS2} - \lambda_{J}I_{RT} - (\zeta_{R} + \delta_{R} + \mu_{H})I_{RT},$$

$$T'_{HT} = \zeta_{T}I_{HT} + \zeta_{R}I_{RT} - \xi\lambda_{T}T_{HT} - \lambda_{J}T_{HT} - \mu_{H}T_{HT},$$

$$E'_{HS} = \lambda_{J}(S_{H} + T_{HT} + \psi T_{HS}) + \zeta_{T1}I_{ST} + \zeta_{R1}I_{RS1} - \eta_{1}\lambda_{T}E_{HS}$$

$$- (\alpha_{1} + \mu_{H})E_{HS},$$

$$I'_{HS} = \alpha_{1}E_{HS} + \zeta_{T2}I_{RS2} + \zeta_{T3}I_{TS} - \eta_{2}\lambda_{T}I_{HS} - (\zeta_{S} + \delta_{S} + \mu_{H})I_{HS},$$

$$T'_{HS} = \zeta_{S}I_{HS} - \lambda_{T}T_{HS} - \psi\lambda_{J}T_{HS} - \mu_{H}T_{HS},$$

$$E'_{TS} = (1 - m)\eta_{1}\lambda_{T}E_{HS} + \lambda_{J}E_{HT} + \zeta_{TS}V_{TS}\lambda_{T} - (1 - \pi_{2})\lambda_{T}E_{TS}$$

$$- (\alpha_{2} + \kappa_{2} + \mu_{H})E_{TS},$$

$$I'_{ST} = m\eta_{1}\lambda_{T}E_{HS} + \lambda_{J}I_{HT} + \lambda_{J}I_{RT} + \kappa_{2}E_{TS} - (\zeta_{T1} + \sigma + \chi_{1}\delta_{T} + \mu_{H})I_{ST},$$

$$I'_{RS1} = (1 - \pi_{2})\lambda_{T}E_{TS} - (\alpha_{3} + \zeta_{R1} + \tau_{1}\delta_{R} + \mu_{H})I_{RS1},$$

$$E'_{ST} = (1 - f)\eta_{2}\lambda_{T}I_{HS} + \alpha_{2}E_{TS} - (1 - \pi_{3})\lambda_{T}E_{ST} - (\zeta_{S1} + \kappa_{3} + v_{1}\delta_{S} + \mu_{H})E_{ST},$$

$$I'_{RS2} = (1 - \pi_{3})\lambda_{T}E_{ST} + \alpha_{3}I_{RS1} - (\zeta_{T3} + \zeta_{S2} + \tau_{2}\delta_{R} + v_{2}\delta_{S} + \mu_{H})I_{RS2},$$

$$I'_{TS} = f\eta_{2}\lambda_{T}I_{HS} + \kappa_{3}E_{ST} + \sigma_{1}S_{T} - (\zeta_{T3} + \zeta_{S3} + \chi_{2}\delta_{T} + v_{3}\delta_{S} + \mu_{H})I_{TS},$$

$$L' = N_{e}\gamma(I_{HS} + E_{ST} + I_{RS2} + I_{TS}) - \mu_{L}L,$$

$$S'_{S} = \Lambda_{S} - \lambda_{L}S_{S} - \mu_{S}S_{S},$$

$$I'_{S} = \lambda_{L}S_{S} - \mu_{S}I_{S},$$

$$J' = \phi I_{S} - \mu_{J}J,$$

$$\lambda_{T} = \frac{\beta_{T}(I_{HT} + \Theta_{RT}I_{RT} + \Theta_{RS1}I_{RS1} + \Theta_{RS2}I_{RS2} + \Pi_{1}I_{ST} + \Pi_{2}I_{TS})}{N_{H}},$$

$$\lambda_{J} = \frac{\beta_{J}J}{J_{0} + \epsilon J}, \qquad \lambda_{L} = \frac{\beta_{L}L}{L_{0} + \epsilon L}.$$
(2.4)

Table 1: Description of state variables of the model (2.3)

State Variables	Description	
$S_H(t)$	Susceptible human population	
V_T	Human population vaccinated with BCG	
V_{TS}	Human population vaccinated with BCG and exposed to schistos-	
	omiasis	
$E_{HT}(t)$	Human population with dormant TB	
$I_{HT}(t)$	Human population with virulent TB	
$I_{RT}(t)$	Human population exogenously infected with TB	
$T_{HT}(t)$	Human population treated for TB	
$E_{HS}(t)$	Human population unprotected against schistosomiasis	
$I_{HS}(t)$	Human population contaminated with schistosomiasis	
$T_{HS}(t)$	Human population cured of schistosomiasis	
$E_{TS}(t)$	Human population unprotected against both TB and schistosomiasis	
$I_{ST}(t)$	Human population with active TB and unprotected against schistosomiasis	
$I_{RS1}(t)$	Human population externally infected with TB and unprotected against	
	schistosomiasis	
$E_{ST}(t)$	Human population unprotected against TB and virulent schistosomiasis	
$I_{RS2}(t)$	Human population externally infected with TB and active	
	schistosomiasis	
$I_{TS}(t)$	Human population with contagious TB and active schistosomiasis	
L(t)	Miracidia (parasite larvae immediately after hatching from the eggs)	
	population	
$S_S(t)$	Susceptible snail populace	
$I_S(t)$	Snail populace contaminated with miracidia in the marine environment	
J(t)	Cercariae (larvae in the water that pierces the human skin) populace	

2.1 Fundamental Properties of the Vaccination Model

2.1.1 Positivity of Solutions and Boundedness of Solutions

As regards the extended TB-schistosomiasis transmission model (2.3) with BCG vaccination to be epidemiologically consequential, it is crucial to prove that all trajectories with initial data that are positive will remain positive permanently and the biologically suitable region is bound to stay positively-invariant for all time.

Table 2: Description of state variables of the model (2.3)

Parameters	Description		
Λ_H	Human recruitment rate		
μ_H	Human natural mortality rate		
β_T	TB transmission rate		
ξ	Reduced rate of infection with TB, $\xi \leq 1$		
f, m, p	Proportion of fast progressors to TB		
π_1,π_2,π_3	Exogenous re-infection rates, where $0 \le \pi_1, \pi_2, \pi_3 \le 1$		
$\kappa_1, \kappa_2, \kappa_3$	Endogenous reactivation rates		
$\zeta_T, \zeta_{T1}, \zeta_{T2}, \zeta_{T3}, \zeta_R, \zeta_{R1}$	Therapeutic rates for TB		
δ_T, δ_R	TB-influenced human death rates		
ψ	Lowered rate of contagion with schistosomiasis		
α_1	Advancement rate from dormant to virulently tainted with		
	schistosomiasis		
α_2	Advancement rate from unprotected against both TB/schistosomiasis		
	to unprotected against TB/virulent schistosomiasis		
α_3	Advancement rate from externally re-tainted with TB-		
	/unprotected against schistosomiasis to externally re-tainted with TB-		
	/virulent schistosomiasis		
$\zeta_S, \zeta_{S1}, \zeta_{S2}, \zeta_{S3}$	Therapeutic rates for schistosomiasis		
δ_S	Schistosomiasis-influenced human mortality rate		
σ	Advancement rate from virulent TB/unprotected against schistosomiasis		
	to virulent TB/virulent schistosomiasis		
χ_1,χ_2	Modification parameters for elevated TB mortality as a consequence		
	of co-infection		
η_1,η_2	Adjustment parameters for the rate at which humans with		
	dormant and virulent schistosomiasis are infected with TB		
$\Theta_{RT}, \Theta_{RS1}, \Theta_{RS2}$	Adjustment parameters for comparative infectiousness of re-infected		
	humans		
Π_1,Π_2	Adjustment parameters for comparative contagiousness of humans		
	with virulent TB and dormant/virulent schistosomiasis		
$ au_1, au_2$	Modification parameters for elevated TB deaths to external re-tainting		
	as a result of co-infection		
v_1, v_2, v_3	Adjustment parameters for schistosomiasis-induced deaths		
Λ_S	Enrollment rate for snail population		
μ_S	Snail mortality rate		
ϵ	Growth velocity limitation		
L_0	Saturation constant for the miracidia		
eta_L	Miracidial contagion rate		
N_e	Statistic of eggs excreted by people		

Parameters	Description
ω	Proportion unvaccinated with BCG against TB
$1-\epsilon_1$	Reduction in BCG vaccine efficacy
$ heta_V$	Vaccine waning
ζ_{TS}	Impact of schistosomiasis on the BCG protection against TB, $\zeta_{TS} \geq 1$

Table 3: Description of state variables of the model (2.3)

Theorem 2.1. Allow the primary input for the TB-schistosomiasis co-infection model (2.3) be given as $S_H(0) > 0$, $V_T(0) > 0$, $V_{TS}(0) > 0$, $E_{HT}(0) > 0$, $I_{HT}(0) > 0$, $I_{RT}(0) > 0$, $T_{HT}(0) > 0$, $E_{HS}(0) > 0$, $I_{HS}(0) > 0$, $I_{HS}(0)$

Proof. Let $t_1 = \sup\{t > 0 : S_H(0) > 0, \ V_T(0) > 0, \ V_{TS}(0) > 0, \ E_{HT}(0) > 0, \ I_{HT}(0) > 0, \ I_{RT}(0) > 0, \ T_{HT}(0) > 0, \ I_{HS}(0) > 0, \ I_{HS}(0) > 0, \ I_{HS}(0) > 0, \ I_{ST}(0) > 0,$

$$\frac{dS_H(t)}{dt} = \omega \Lambda_H + \theta_V V_T - (\lambda_T + \lambda_J + \mu_H) S_H(t), \qquad (2.5)$$

It ensues from (2.5) above that

$$\frac{dS_H(t)}{dt} \ge \omega \Lambda_H - (\lambda_T + \lambda_J + \mu_H) S_H(t), \tag{2.6}$$

which can be re-expressed as

$$\frac{d}{dt} \left[S_H(t) \exp\left\{ \mu_H t + \int_0^t (\lambda_T(\tau) + \lambda_J(\tau)) d\tau \right\} \right]
\geq \omega \Lambda_H \exp\left\{ \mu_H t + \int_0^t (\lambda_T(\tau) + \lambda_J(\tau)) d\tau \right\}.$$
(2.7)

Therefore, integrating (2.7) with respect to $t \in [0, t_1]$, we get

$$S_{H}(t_{1}) \exp\left\{\mu t_{1} + \int_{0}^{t_{1}} (\lambda_{T}(\tau) + \lambda_{J}(\tau)) d\tau\right\} - S_{H}(0)$$

$$\geq \int_{0}^{t_{1}} \omega \Lambda_{H} \left[\exp\left\{\mu_{H}y + \int_{0}^{y} (\lambda_{T}(\tau) + \lambda_{J}(\tau)) d\tau\right\}\right] dy,$$
(2.8)

Therefore,

$$S_{H}(t_{1}) \geq S_{H}(0) \exp\left[-\mu_{H}t_{1} - \int_{0}^{t_{1}} (\lambda_{T}(\tau) + \lambda_{J}(\tau))d\tau\right]$$

$$+ \left[\exp\left\{-\mu_{H}t_{1} - \int_{0}^{t_{1}} (\lambda_{T}(\tau) + \lambda_{J}(\tau))d\tau\right\}\right]$$

$$\times \int_{0}^{t_{1}} \omega\Lambda_{H}\left[\exp\left\{\mu_{H}y + \int_{0}^{y} (\lambda_{T}(\tau) + \lambda_{J}(\tau))d\tau\right\}\right]dy > 0.$$
(2.9)

Thus $S_H(t) > 0, \forall t > 0.$

Similarly, considering the second to the twentieth equations of model (2.3), which can be rewritten as $V_T(t) > 0$, $V_{TS}(t) > 0$, $E_{HT}(t) > 0$, $I_{HT} > 0$, $I_{RT}(t) > 0$, $T_{HT}(t) > 0$, $E_{HS}(t) > 0$, $I_{HS}(t) > 0$, and $I_{HS}(t) > 0$, $I_{HS}(t) > 0$.

Therefore, the positivity for every state variable in model (2.3) for all time has been entrenched.

Theorem 2.2. Let $(S_H(t), V_T(t), V_{TS}(t), E_{HT}(t), I_{HT}(t), I_{RT}(t), T_{HT}(t), E_{HS}(t), I_{HS}(t), T_{HS}(t), E_{TS}(t), I_{ST}(t), I_{RS1}(t), E_{ST}(t), I_{RS2}(t), I_{TS}(t), L(t), S_S(t), I_S(t), J(t))$ be solutions of the system (2.3) wth initial conditions and the biologically suitable region given by the set $\mathcal{D}_V = \mathcal{D}_H \times \mathcal{D}_L \times \mathcal{D}_S \times \mathcal{D}_J \subset \mathbb{R}^{16}_+ \times \mathbb{R}^1_+ \times \mathbb{R}^2_+ \times \mathbb{R}^1_+ \subset \mathbb{R}^{20}_+$ where:

$$\mathcal{D}_{H} = \{ (S_{H}, V_{T}, V_{TS}, E_{HT}, I_{HT}, I_{RT}, T_{HT}, E_{HS}, I_{HS}, T_{HS}, E_{TS}, I_{ST}, I_{RS1}, E_{ST}, I_{RS2}, I_{TS}) \in \mathbb{R}^{16}_{+} : N_{H} \leq \frac{\Lambda_{H}}{\mu_{H}} \}$$

$$\mathcal{D}_{L} = \{ L \in \mathbb{R}^{1}_{+} : L \leq \frac{N_{e} \gamma \Lambda_{H}}{\mu_{L} \mu_{H}} \}$$

$$\mathcal{D}_{S} = \{ (S_{S}, I_{S}) \in \mathbb{R}^{2}_{+} : N_{S} \leq \frac{\Lambda_{S}}{\mu_{S}} \}$$

$$\mathcal{D}_{J} = \{ J \in \mathbb{R}^{1}_{+} : J \leq \frac{\phi \Lambda_{S}}{\mu_{J} \mu_{S}} \}$$

is positively-invariant and pulls all the positive solutions of the model (2.3).

Proof. Summing up the right hand side of the vector field for the population of people in (2.3), gives

$$\frac{dN_H}{dt} = \Lambda_H - \mu_h N - (\delta_T I_{HT} + \delta_R I_{RT} + \delta_S I_{HS} + \chi_1 \delta_T I_{ST} + \tau_1 \delta_R I_{RS1} + v_1 \delta_S E_{ST} + (\tau_2 \delta_R + v_2 \delta_S) I_{RS2} + (\chi_2 \delta_T + v_3 \delta_S) I_{TS}.$$
(2.10)

From (2.10), thence $\frac{dN_H}{dt} \leq \Lambda_H - \mu_H N_H$. Therefore, $\frac{dN_H}{dt} \leq 0$ if $N_H(t) \geq \frac{\Lambda_H}{\mu_H}$. Employing the acceptable comparison theorem by [29], we reveal that.

$$N_H(t) \le N_H(0)e^{-\mu_H t} + \frac{\Lambda_H}{\mu_H}(1 - e^{-\mu_H t}). \tag{2.11}$$

In particular, if $N_H(0) \leq \frac{\Lambda_H}{\mu_H}$, then $N_H(t) \leq \frac{\Lambda_H}{\mu_H}$ for all t > 0. Hence, the set \mathcal{D}_H is positively invariant.

Furthermore, if $N_H(0) > \frac{\Lambda_H}{\mu_H}$, then either the solutions enter the domain \mathcal{D}_H in finite time or $N_H(t)$ asymptotically nears $\frac{\Lambda_H}{\mu_H}$ as $t \to \infty$. Therefore, the domain \mathcal{D}_H attracts all trajectories in \mathbb{R}^{16}_+ .

For the miracidia concentration, from (2.3), it follows that

$$\frac{dL}{dt} = N_e \gamma (I_{HS} + E_{ST} + I_{RS2} + I_{TS}) - \mu_L L. \tag{2.12}$$

From (2.12), which follows that $\frac{dL}{dt} \leq \frac{N_e \gamma \Lambda_H}{\mu_H} - \mu_L L$ since $N_H = S_H + V_T + V_{TS}$, $E_{HT} + I_{HT} + I_{RT} + T_{HT} + E_{HS} + I_{HS} + E_{TS} + I_{ST} + I_{RS1} + E_{ST} + I_{RS2} + I_{TS} \leq \frac{\Lambda_H}{\mu_H} \Longrightarrow I_{HS} + E_{TS} + I_{RS2} + I_{TS} \leq \frac{\Lambda_H}{\mu_H}$. Hence, $\frac{dL}{dt} \leq 0$ if $L(t) \geq \frac{N_e \gamma \Lambda_H}{\mu_L \mu_H}$. Employing the acceptable comparison theorem by [29], we show that $L(t) \leq L(0)e^{-\mu_L t} + \frac{N_e \gamma \Lambda_H}{\mu_L \mu_H} (1 - e^{-\mu_L t})$. Specifically, if $L(0) \leq \frac{N_e \gamma \Lambda_H}{\mu_L \mu_H}$, thus $L(t) \leq \frac{N_e \gamma \Lambda_H}{\mu_L \mu_H}$ for every t > 0. Thus, the set \mathcal{D}_L is positively constant. Furthermore, if $L(0) > \frac{N_e \gamma \Lambda_H}{\mu_L \mu_H}$, then the solutions either penetrate the domain \mathcal{D}_L in finite time or L(t) asymptotically approaches $\frac{N_e \gamma \Lambda_H}{\mu_L \mu_H}$ as $t \to \infty$. Therefore, the domain \mathcal{D}_L attracts all trajectories in \mathbb{R}^1_+ .

For the snail populace, summing up the right hand side of the vector field of the snail population in (2.3), leads to

$$\frac{dN_S}{dt} = \Lambda_S - \mu_S N_S. \tag{2.13}$$

From (2.13), it follows that $\frac{dN_S}{dt} \leq 0$ if $N_S(t) \geq \frac{\Lambda_S}{\mu_S}$. It indicates that $N_S(t) = N_S(0)e^{-\mu_S t} + \frac{\Lambda_S}{\mu_S}(1-e^{-\mu_S t})$. Therefore the $\limsup_{t\to\infty} N_S(t) = \frac{\Lambda_S}{\mu_S}$. Specifically, if $N_S(0) \leq \frac{\Lambda_S}{\mu_S}$, thus $N_S(t) \leq \frac{\Lambda_S}{\mu_S}$ for all t>0. Thus, the set \mathcal{D}_S is positively constant. Furthermore, if $N_S(0) > \frac{\Lambda_S}{\mu_S}$, then the solutions either enter the domain \mathcal{D}_S in finite time or $N_S(t)$ asymptotically nears $\frac{\Lambda_S}{\mu_S}$ as $t\to\infty$. Therefore, the domain \mathcal{D}_S pulls all trajectories in \mathbb{R}^2_+ .

For the clustering of the cercariae, considering the right hand side of the vector field J in (2.3), yields

$$\frac{dJ}{dt} = \phi I_S - \mu_J J. \tag{2.14}$$

From (2.14), $\frac{dJ}{dt} = \phi I_S - \mu_J J$ which follows that $\frac{dJ}{dt} \leq \frac{\phi \Lambda_S}{\mu_S} - \mu_J J$ since $N_S = S_S + I_S \leq \frac{\Lambda_S}{\mu_S} \Longrightarrow I_S \leq \frac{\Lambda_S}{\mu_S}$. Hence, $\frac{dJ}{dt} \leq 0$ if $J(t) \geq \frac{\phi \Lambda_S}{\mu_J \mu_S}$. Using the accepted comparison theorem by [29], we arrive at $J(t) \leq J(0)e^{-\mu_J t} + \frac{\phi \Lambda_S}{\mu_J \mu_S}(1 - e^{-\mu_J t})$. Specifically, if $J(0) \leq \frac{\phi \Lambda_S}{\mu_J \mu_S}$, then $J(t) \leq \frac{\phi \Lambda_S}{\mu_J \mu_S}$ for all t > 0. Therefore,

the set \mathcal{D}_J is positively constant. Furthermore, if $J(0) > \frac{\phi \Lambda_S}{\mu_J \mu_S}$, then either the orbits penetrate the domain \mathcal{D}_J in finite time or J(t) asymptotically approaches $\frac{\phi \Lambda_S}{\mu_J \mu_S}$ as $t \to \infty$. Therefore, the domain \mathcal{D}_J pulls all solutions in \mathbb{R}^1_+ .

From the above, we have shown that $\mathcal{D}_H, \mathcal{D}_L, \mathcal{D}_S$ and \mathcal{D}_J are positively invariant and since $\mathcal{D}_V = \mathcal{D}_H \times \mathcal{D}_L \times \mathcal{D}_S \times \mathcal{D}_J$, it implies that the domain \mathcal{D}_V is positively-invariant and an attractor, so that no solution leaves through any boundary of \mathcal{D}_V .

es through any boundary of
$$\mathcal{D}_V$$
.
$$\mathcal{D}_V = \begin{cases} (S_H, V_T, V_{TS}, E_{HT}, I_{HT}, I_{RT}, T_{HT}, E_{HS}, I_{HS}, T_{HS}, E_{TS}, I_{ST}, I_{RS1}, \\ E_{ST}, I_{RS2}, I_{TS}) \in \mathbb{R}_+^{16} : N_H \leq \frac{\Lambda_H}{\mu_H} \\ L \in \mathbb{R}_+^1 : L \leq \frac{N_e \gamma \Lambda_H}{\mu_L \mu_H} \\ (S_S, I_S) \in \mathbb{R}_+^2 : N_S \leq \frac{\Lambda_S}{\mu_S} \\ J \in \mathbb{R}_+^1 : J \leq \frac{\phi \Lambda_S}{\mu_J \mu_S} \end{cases}$$

It is therefore enough to study the dynamics of the solutions generated by the system (2.3) in \mathcal{D}_V . We conclude, therefore, that the model (2.3) is both mathematically and epidemiologically well-posed. \square

3 Mathematical Analysis of the Co-infection Model with Vaccination

3.1 Local Asymptotic Stability of Disease-Free Equilibrium (DFE)

The model system (2.3) has a DFE given by

It is revealed via the next-generation operator approach [57], that the associated effective reproduction number of the model (2.3), \mathcal{R}_{TS}^{V} , is given by

$$\mathcal{R}_{TS}^{V} = \max\left\{\mathcal{R}_{HT}^{V}, \mathcal{R}_{HS}\right\},\tag{3.1}$$

$$\mathcal{R}_{HT}^{V} = \frac{\beta_T \left(\theta_V (\kappa_1 + p\mu_H) + \mu_H ((1 - (1 - \omega)\epsilon_1)\kappa_1 + p\omega\mu_H)\right)}{(\kappa_1 + \mu_H)(\zeta_T + \delta_T + \mu_H)(\theta_V + \mu_H)},$$

$$\mathcal{R}_{HS} = \sqrt{\frac{\alpha_1 \beta_J \beta_L \Lambda_H \Lambda_S N_e \gamma \phi}{J_0 L_0 \mu_H \mu_J \mu_L \mu_S^2 (\alpha_1 + \mu_H)(\zeta_S + \delta_S + \mu_H)}}$$

represent the effective reproduction number for TB cum schistosomiasis, respectively.

Utilising the Second Theorem in [57], the subsequent consequence is established:

Lemma 3.1. The DFE \mathcal{E}_o is locally asymptotically stable (LAS) in \mathcal{D} if $\mathcal{R}_{TS}^V < 1$ and unstable if $\mathcal{R}_{TS}^V > 1$.

The threshold quantity, \mathcal{R}_{TS}^{V} , is a measure of the average number of secondary infections engendered by a single infected person in a wholly vulnerable population, where a fraction of the vulnerable human population is vaccinated using an imperfect TB (BCG) vaccine.

3.2 Backward Bifurcation Analysis

Theorem 3.1. If $\mathcal{R}_{TS}^V < 1$ and the coefficients of bifurcation a > 0 and b > 0, consequently (2.3) displays a bifurcation that is backward in nature at $\mathcal{R}_{TS}^V = 1$, contrarily the system displays a bifurcation that is forward at $\mathcal{R}_{TS}^V = 1$.

Proof:

The existence of backward bifurcation is investigated using the *Center Manifold Theory* as espoused by [10]. Allow $S_H = x_1$, $V_T = x_2$, $V_{TS} = x_3$, $E_{HT} = x_4$, $I_{HT} = x_5$, $I_{RT} = x_6$, $T_{HT} = x_7$, $E_{HS} = x_8$, $I_{HS} = x_9$, $T_{HS} = x_{10}$, $E_{TS} = x_{11}$, $I_{ST} = x_{12}$, $I_{RS1} = x_{13}$, $E_{ST} = x_{14}$, $I_{RS2} = x_{15}$, $I_{TS} = x_{16}$, $L = x_{17}$, $S_S = x_{18}$, $I_S = x_{19}$ and $J = x_{20}$, let $N_H = \sum_{i=1}^{16} x_i$; therefore the model (2.3) is re-expressed as

$$\begin{split} \dot{x}_1 &\equiv f_1 = \omega \Lambda_H + \theta_V x_2 - \lambda_T x_1 - \lambda_J x_1 - \mu_H x_1, \\ \dot{x}_2 &\equiv f_2 = (1 - \omega) \Lambda_H - \lambda_J x_2 - (1 - \epsilon_1) \lambda_T x_2 - Q_1 x_2 \\ \dot{x}_3 &\equiv f_3 = \lambda_J x_2 - \zeta_T s \lambda_T x_3 - \mu_H x_3, \\ \dot{x}_4 &\equiv f_4 = (1 - p) \lambda_T (x_1 + \xi x_7 + x_{10}) + (1 - \epsilon_1) \lambda_T x_2 + \zeta_{S1} x_{14} \\ &\quad - (1 - \pi_1) \lambda_T x_4 - \lambda_J x_4 - Q_2 x_4, \\ \dot{x}_5 &\equiv f_5 = p \lambda_T (x_1 + \xi x_7 + x_{10}) + \kappa_1 x_4 + \zeta_{S3} x_{16} - \lambda_J x_5 - Q_3 x_5, \\ \dot{x}_6 &\equiv f_6 = (1 - \pi_1) \lambda_T x_4 + \zeta_{S2} x_{15} - \lambda_J x_6 - Q_4 x_6, \\ \dot{x}_7 &\equiv f_7 = \zeta_T x_5 + \zeta_R x_6 - \xi \lambda_T x_7 - \lambda_J x_7 - \mu_H x_7, \\ \dot{x}_8 &\equiv f_8 = \lambda_J (x_1 + x_7 + \psi x_{10}) + \zeta_{T1} x_{12} + \zeta_{R1} x_{13} - \eta_1 \lambda_T x_8 \\ &\quad - Q_5 x_8, \\ \dot{x}_9 &\equiv f_9 = \alpha_1 x_8 + \zeta_T 2 x_{15} + \zeta_T 3 x_{16} - \eta_2 \lambda_T x_9 - Q_6 x_9, \\ \dot{x}_{10} &\equiv f_{10} = \zeta_S x_9 - \lambda_T x_{10} - \psi \lambda_J x_{10} - \mu_H x_{10}, \\ \dot{x}_{11} &\equiv f_{11} = (1 - m) \eta_1 \lambda_T x_8 + \lambda_J x_4 + \zeta_T s \lambda_T x_3 - (1 - \pi_2) \lambda_T x_{11} \\ &\quad - Q_7 x_{11}, \\ \dot{x}_{12} &\equiv f_{12} = m \eta_1 \lambda_T x_8 + \lambda_J x_5 + \lambda_J x_6 + \kappa_2 x_{11} - Q_8 x_{12}, \\ \dot{x}_{13} &\equiv f_{13} = (1 - \pi_2) \lambda_T x_{11} - Q_9 x_{13}, \\ \dot{x}_{14} &\equiv f_{14} = (1 - f) \eta_2 \lambda_T x_9 + \alpha_2 x_{11} - (1 - \pi_3) \lambda_T x_{14} - Q_{10} x_{14}, \\ \dot{x}_{15} &\equiv f_{15} = (1 - \pi_3) \lambda_T x_{14} + \alpha_3 x_{13} - Q_{11} x_{15}, \\ \dot{x}_{16} &\equiv f_{16} = f \eta_2 \lambda_T x_9 + \kappa_3 x_{14} + \sigma x_{12} - Q_{12} x_{16}, \\ \dot{x}_{17} &\equiv f_{17} &= N_e \gamma (x_9 + x_{14} + x_{15} + x_{16}) - \mu_L x_{17}, \\ \dot{x}_{18} &\equiv f_{18} &= \Lambda_S - \lambda_L x_{18} - \mu_S x_{18}, \\ \dot{x}_{19} &\equiv f_{19} &= \lambda_L x_{18} - \mu_S x_{19}, \\ \dot{x}_{20} &\equiv f_{20} &= \phi x_{19} - \mu_J x_{20}. \end{split}$$

Therefore the forces of infection associated with the model (3.2) are:

$$\lambda_{T} = \frac{\beta_{T}(x_{5} + \Theta_{RT}x_{6} + \Theta_{RS1}x_{13} + \Theta_{RS2}x_{15} + \Pi_{1}x_{12} + \Pi_{2}x_{16})}{\sum_{i=1}^{16} x_{i}}$$

$$\lambda_{J} = \frac{\beta_{J}x_{20}}{J_{0} + \epsilon x_{20}},$$

$$\lambda_{L} = \frac{\beta_{L}x_{17}}{L_{0} + \epsilon x_{17}},$$

$$Q_1 = \theta_V + \mu_H$$
, $Q_2 = \kappa_1 + \mu_H$, $Q_3 = \zeta_T + \delta_T + \mu_H$, $Q_4 = \zeta_R + \delta_R + \mu_H$, $Q_5 = \alpha_1 + \mu_H$,

 $Q_{6} = \zeta_{S} + \delta_{S} + \mu_{H}, \ Q_{7} = \alpha_{2} + \kappa_{2} + \mu_{H}, \ Q_{8} = \zeta_{T1} + \sigma + \chi_{1}\delta_{T} + \mu_{H}, \ Q_{9} = \alpha_{3} + \zeta_{R1} + \tau_{1}\delta_{R} + \mu_{H}, \ Q_{10} = \zeta_{S1} + \kappa_{3} + v_{1}\delta_{S} + \mu_{H}, \ Q_{11} = \zeta_{T2} + \zeta_{S2} + \tau_{2}\delta_{R} + v_{2}\delta_{S} + \mu_{H}, \ \text{and} \ Q_{12} = \zeta_{T3} + \zeta_{S3} + \chi_{2}\delta_{T} + v_{3}\delta_{S} + \mu_{H}.$

The system (3.2), at the DFE with $\beta_T = \beta_T^*$, has a Jacobian given by:

$$J_{\beta_T^*} = J(\mathcal{E}_0)|_{\beta_T^*} = \begin{pmatrix} J_{11}(10 \times 10) & J_{12}(10 \times 10) \\ J_{21}(10 \times 10) & J_{22}(10 \times 10) \end{pmatrix}, \tag{3.3}$$

and

$$A_{1} = \frac{(1-p)(\theta_{V} + \omega\mu_{H}) + \mu_{H}(1-\omega)(1-\epsilon_{1})}{\theta_{V} + \mu_{H}},$$

$$B_{1} = \frac{\theta_{V} + \omega\mu_{H}}{\theta_{V} + \mu_{H}}, \quad C_{1} = \frac{\mu_{H}(1-\omega)(1-\epsilon_{1})}{\theta_{V} + \mu_{H}},$$

$$D_{1} = \frac{\Lambda_{H}(1-\omega)}{J_{0}(\theta_{V} + \mu_{H})}, \quad E_{1} = \frac{\Lambda_{H}(\theta_{V} + \omega\mu_{H})}{J_{0}\mu_{H}(\theta_{V} + \mu_{H})}, \quad F_{1} = \frac{\Lambda_{S}}{L_{0}\mu_{S}}.$$
(3.8)

Let us view the situation where $\mathcal{R}_{TS}^{V} = 1$. it is presumed that the maximum of

$$\mathcal{R}_{TS}^{V} = \max\left\{\mathcal{R}_{HT}^{V}, \mathcal{R}_{HS}\right\} = \mathcal{R}_{HT}^{V}.$$
(3.9)

Solving for $\beta_T = \beta_T^*$ from $\mathcal{R}_{HT}^V = 1$ gives

$$\beta_T = \beta_T^* = \frac{(\kappa_1 + \mu_H)(\zeta_T + \delta_T + \mu_H)(\theta_V + \mu_H)}{\theta_V(\kappa_1 + p\mu_H) + \mu_H((1 - (1 - \omega)\epsilon_1)\kappa_1 + p\omega\mu_H)}$$
(3.10)

Matrix $J_{\beta_T^*}$ possesses a right eigenvector revealed by $\mathbf{w} = (\omega_1, \omega_2, ..., \omega_{20})^T$, where

$$w_{1} = -\frac{(\beta_{T}^{*}(Q_{1}B_{1} + \theta_{V}C_{1})w_{5} + \beta_{J}(\theta_{V}D_{1} + Q_{1}E_{1})w_{20})}{Q_{1}},$$

$$w_{2} = -\frac{(\beta_{T}^{*}C_{1}w_{5} + \beta_{J}D_{1}w_{20})}{Q_{1}}, \quad w_{3} = \frac{\beta_{J}D_{1}w_{20}}{\mu_{H}}, \quad w_{4} = \frac{\beta_{T}^{*}A_{1}}{Q_{2}(Q_{3} - p\beta_{T}^{*}B_{1})},$$

$$w_{5} = \frac{Q_{2}}{\beta_{T}^{*}\kappa_{1}A_{1}}, w_{6} = 0, \quad w_{7} = \frac{\zeta_{T}w_{5}}{\mu_{H}}, \quad w_{8} = \frac{\beta_{J}E_{1}w_{20}}{Q_{5}}, \quad w_{9} = \frac{\alpha_{1}\beta_{J}E_{1}w_{20}}{\mu_{H}Q_{5}Q_{6}},$$

$$w_{10} = \frac{\alpha_{1}\beta_{J}\zeta_{S}E_{1}w_{20}}{\mu_{H}Q_{5}Q_{6}}, \quad w_{11} = w_{12} = w_{13} = w_{14} = w_{15} = w_{16} = 0,$$

$$w_{17} = \frac{\mu_{J}\mu_{S}w_{20}}{\beta_{L}\phi F_{1}}, \quad w_{18} = -\frac{\mu_{J}w_{20}}{\phi}, \quad w_{19} = \frac{\mu_{J}w_{20}}{\phi}, \quad w_{20} = w_{20} > 0.$$

$$(3.11)$$

where $w_4 > 0, w_5 > 0$.

In addition, $J_{\beta_T^*}$ possesses a left eigenvector $\mathbf{v} = (\nu_1, \nu_2,, \nu_{20})$ fulfilling $\mathbf{v.w} = \mathbf{1}$, with

$$\nu_{1} = \nu_{2} = \nu_{3} = 0, \nu_{4} = \frac{\kappa_{1}}{Q_{2}(Q_{3} - p\beta_{T}^{*}B_{1})}, \nu_{5} = \frac{Q_{2}}{\beta_{T}^{*}\kappa_{1}A_{1}},$$

$$\nu_{6} = \frac{\beta_{T}^{*}\Theta_{RT}(A_{1}\nu_{4} + pB_{1}\nu_{5})}{Q_{4}}, \nu_{7} = 0, \nu_{8} = \frac{\mu_{J}\nu_{20}}{\beta_{J}E_{1}}, \nu_{9} = \frac{\mu_{J}Q_{5}\nu_{20}}{\alpha_{1}\beta_{J}E_{1}},$$

$$\nu_{10} = 0, \nu_{11} = \frac{\kappa_{2}\nu_{12} + \alpha_{2}\nu_{14}}{Q_{7}},$$

$$\nu_{12} = \frac{\beta_{T}^{*}\Pi_{1}(A_{1}\nu_{4} + pB_{1}\nu_{5}) + \zeta_{T1}\nu_{8} + \sigma\nu_{16}}{Q_{8}},$$

$$\nu_{13} = \frac{\beta_{T}^{*}\Theta_{RS1}(A_{1}\nu_{4} + pB_{1}\nu_{5}) + \zeta_{R1}\nu_{8} + \alpha_{3}\nu_{15}}{Q_{9}},$$

$$\nu_{14} = \frac{\zeta_{S1}\nu_{4} + \kappa_{3}\nu_{16} + N_{e}\gamma\nu_{17}}{Q_{10}},$$

$$\nu_{15} = \frac{\beta_{T}^{*}\Theta_{RS2}(A_{1}\nu_{4} + pB_{1}\nu_{5}) + \zeta_{S2}\nu_{6} + \zeta_{T2}\nu_{9} + N_{e}\gamma\nu_{17}}{Q_{11}},$$

$$\nu_{16} = \frac{\beta_{T}^{*}\Pi_{2}(A_{1}\nu_{4} + pB_{1}\nu_{5}) + \zeta_{T3}\nu_{9} + N_{e}\gamma\nu_{17}}{Q_{12}},$$

$$\nu_{17} = \frac{\beta_{L}\phi F_{1}\nu_{20}}{\mu_{L}\mu_{S}}, \nu_{18} = 0, \nu_{19} = \frac{\phi\nu_{20}}{\mu_{S}}, \nu_{20} = \nu_{20} > 0,$$

where $\nu_4 > 0, \nu_5 > 0$.

Furthermore, employing the Center Manifold Theory as presented by [10], we proceed to calculate the linked non-zero partial derivatives of the right hand sides of the transformed system (3.2), (considered at the point where there is without infection with $\beta_T = \beta_T^*$) that the linked coefficients of bifurcation, a and b, are described as

$$a = \sum_{k,i,j=1}^{n} v_k w_i w_j \frac{\partial^2 f_k}{\partial x_i \partial x_j}(0,0), \quad \text{and} \quad b = \sum_{k,i=1}^{n} v_k w_i \frac{\partial^2 f_k}{\partial x_i \partial \beta_T^*}(0,0), \quad (3.13)$$

$$\begin{split} a &= \frac{2\beta_T^n \mu_H}{\Lambda_H} \Big[(1-\pi_1)\Theta_{RT} \Big(\frac{A_1\nu_4 + pB_1\nu_5}{Q_4} \Big) w_4 w_5 + ((1-p)\nu_4 + p\nu_5) \Big(\frac{\zeta_5\alpha_1\beta_J^*E_1}{\mu_H Q_5Q_6} w_5 w_{20} + \frac{\xi\zeta_T}{\mu_H} w_5^2 \Big) \Big] \\ &+ \frac{2\beta_T^*}{Q_2(Q_3 - p\beta_T^*B_1)} \Big[\frac{(1-p)}{Q_1(Q_3 - \beta_T B_1)} \Big(\frac{\beta_T \omega \mu_H^2}{\theta_V + \mu_H} \Big(\mu_H (1-\omega)(1-\epsilon_1) - A_1(\theta_V + \mu_H) \Big) - \mu_H Q_1 Q_3 \Big) \\ &+ \Big(\frac{Q_2Q_3}{\theta_V + \omega \mu_H} \Big(\mu_H (1-\omega)(1-\epsilon_1) - A_1(\theta_V + \mu_H) \Big) \\ &+ 2\mu_H (1-\omega)(1-\epsilon_1) A_1(\theta_V + \mu_H) \Big) \\ &- \Big((\mu_H (1-\omega)(1-\epsilon_1))^2 + (A_1(\theta_V + \mu_H))^2 \Big) \Big) B_1 w_5 (G_1 + G_2) \Big) \\ &+ \frac{\Lambda_H}{J_0 \mu_H} \Big(\frac{\theta_V}{\theta_V + \mu_H} - B_1 \Big) \nu_4 w_5 G_1 + \zeta_{TS} \nu_{11} w_3 w_5 \\ &+ \eta_1 ((1-m)\nu_{11} + m\nu_{12}) w_5 w_8 \\ &+ \eta_2 ((1-f)\nu_{14} + f\nu_{16}) w_5 w_9 \\ &+ (1-\epsilon_1) D_1 \nu_4 w_5 G_2 \Big] \\ &+ \frac{2\beta_J^*}{J_0} \Big[\frac{\zeta_T}{\mu_H} \nu_8 w_5 w_{20} + \psi \nu_8 w_{10} w_{20} \\ &+ \Big(\frac{\kappa_2 \left(\beta_T^* \Pi_1 (A_1 \nu_4 + pB_1 \nu_5) + \zeta_{T1} \nu_8 + \sigma \nu_{16} \right)}{Q_7 Q_8} + \frac{\alpha_2 \nu_{14}}{Q_7} \Big) w_4 w_{20} \Big] \\ &- \frac{2\beta_T^* \mu_H}{\Lambda_H} \Big[\Big((1-p)G_1 + (1-\epsilon_1)G_2 \big) \nu_4 w_5 + (1-\pi_1)\nu_4 w_4 w_5 + \eta_2 \nu_9 w_5 w_9 \Big] \\ &- 2\beta_T^* \Big[\Big((1-p)B_1 + C_1 \Big) \Big(\nu_4 w_5 (w_3 + w_8 + w_9) + \nu_4 w_4 w_5 + \nu_4 w_5^2 + \nu_4 w_4 w_7 \Big) \\ &+ pB_1 \Big(\nu_5 w_5 (w_3 + w_4 + w_8 + w_9) + \nu_5 w_5^2 + \nu_5 w_4 w_7 \Big) + C_1 + \nu_4 w_5^2 + \nu_4 w_5 w_{10} \Big] \\ &- \frac{2\beta_J^*}{J_0} \Big[\Big(\nu_4 w_4 + \nu_5 w_5 + \epsilon E_1 \nu_8 w_{20} \Big) w_{20} \Big] \\ &- \frac{2\beta_L}{J_0} \Big[\Big(\nu_4 w_4 + \nu_5 w_5 + \epsilon E_1 \nu_8 w_{20} \Big) w_{20} \Big] \\ &- \frac{2\beta_L}{J_0} \Big[\nu_{19} w_{17} \Big(\epsilon F_1 w_{17} + w_{19} \Big) \Big]. \end{aligned}$$

where

$$G_1 = \frac{J_1 w_5 + J_2 w_{20}}{Q_1}, \quad G_2 = \frac{J_3 w_5 + J_4 w_{20}}{Q_1},$$

$$J_1 = (\theta_V C_1 + Q_1 B_1) \beta_T^*, \quad J_2 = (\theta_V D_1 + Q_1 E_1) \beta_J^*,$$

$$J_3 = C_1 \beta_T^*, \quad J_4 = D_1 \beta_J^*.$$

Since $Q_3 - p\beta_T^*B_1 > 0$, $\Longrightarrow Q_3 - \beta_T^*B_1 > 0$. However, since $0 , then <math>p\beta_T^*B_1 < \beta_T^*B_1$. This, therefore, implies that $Q_3 - p\beta_T^*B_1 > Q_3 - \beta_T^*B_1 \Longrightarrow (1-p)\beta_T^*B_1 > 0$, and

$$b = (\nu_4 A_1 + \nu_5 p B_1) w_5 \tag{3.15}$$

Clearly b > 0 for every biologically appropriate parameter values.

Since our purpose, herein, is in unveiling the parameter(s), which is(are) liable for maintaining the negativity of the the coefficient of bifurcation, a, that is a < 0, it behoves us to recognize at this point, that [54] entrenched that the comparative rate of contagiousness of externally re-tainted persons is a definite cause of backward bifurcation in TB transmission dynamics. In the same vein, it has also been reported in the literature by [2,3,52] that recontamination is a basis for the phenomenon of the bifurcation that is backward in schistosomiasis epidemic dynamics. A close observation of (3.14) reveals that eradicating the rate of comparative contagiousness of externally re-tainted persons (Θ_{RT}) and the lowered rate of re-contamination with schistosomiasis (ψ) (i.e., $\Theta_{RT} = \psi = 0$) will not completely produce the appropriate outcome of eradicating the backward bifurcation phenomenon resident in a TB-schistosomiasis co-infection model taking into consideration the effect of schistosomiasis infection on the immunogenicity of the BCG vaccine as it affects the use of vaccination as a measure of control against TB infection at population level because the positive part of (3.14) does not completely disappear just as reported in [3]. This, therefore, is indicative that there are some other parameters accountable for this predicament. Additional investigation identifies the adjustment parameter for comparative contagiousness of persons re-tainted with TB (Θ_{RT}) , the treatment rate for schistosomiasis-only infected persons (ζ_S) , the BCG vaccine waning (θ_V) , the impact of schistosomiasis on the BCG protection against TB (ζ_{TS}) , the comparative rates by which persons with dormant schistosomiasis (η_1) and virulent schistosomiasis (η_2) are tainted with TB, correspondingly, the BCG vaccine efficacy (ϵ_1), the treatment rate for TB (ζ_T), the depreciated rate of contagion with schistosomiasis (ψ) , the adjustment parameter for relative contagiousness of persons with virulent TB and dormant schistosomiasis (Π_1), the therapeutic rate for TB for co-infected infected persons (ζ_{T1}) , the advancement rate from infectious TB/unprotected against schistosomiasis to infectious TB/infectious schistosomiasis (σ), and the advancement rate from vulnerable to both TB/schistosomiasis to vulnerable to TB/virulent schistosomiasis (α_2) are accountable for the non-eradication of the backward bifurcation dilemma.

Thus, given the condition that for $\mathcal{R}_{TS}^V = 1$, and $\Theta_{RT} = \zeta_{TS} = \theta_V = \eta_1 = \eta_2 = \zeta_T = \psi = \Pi_1 = \zeta_{T1} = \sigma = \alpha_2 = 0$ and $\epsilon_1 = 1$, the bifurcation parameter a will be negative.

In summary, this research has proved that the comparative rate of contagiousness of humans re-contaminated with TB (Θ_{RT}), the therapeutic rate for schistosomiasis-only infected persons (ζ_S), the BCG vaccine waning (θ_V), the impact of schistosomiasis on the BCG protection against TB (ζ_{TS}), the BCG vaccine waning (θ_V), the comparative rates at which persons with dormant schistosomiasis (η_1) and virulent schistosomiasis (η_2) are tainted with TB, correspondingly, the BCG vaccine efficacy (ϵ_1), the treatment rate for TB (ζ_T), the decreased infection rate with schistosomiasis (ψ), the adjustment parameter for relative contagiousness of persons with virulent TB and dormant schistosomiasis (Π_1), the therapeutic rate for TB for co-infected persons (ζ_{T1}), the advancement rate from infectious TB/vulnerable to schistosomiasis to infectious TB/infectious schistosomiasis (σ), cum the advancement rate from vulnerable to the two diseases (TB/schistosomiasis) to vulnerable to TB/infectious schistosomiasis (σ_2)

instigate backward bifurcation in the disease dynamics of TB alongside BCG vaccination in the company of schistosomiasis.

So, the effective reproduction number, \mathcal{R}_{TS}^V , less than unity, becomes a mandatory but not an adequate situation for the control of the two epidemics.

3.3 Global Asymptotic Stability (GAS) of DFE

A this juncture, we proceed to review the global asymptotic stability of the infection-free equilibrium of a unique case of (2.3) with inconsequential adjustment parameter for comparative infectiousness of humans re-tainted with TB ($\Theta_{RT}=0$), the therapeutic rate for schistosomiasis-only infected persons $(\zeta_S = 0)$, the impact of schistosomiasis on the BCG protection against TB $(\zeta_{TS} = 0)$, the BCG vaccine waning $(\theta_V = 0)$, the comparative rates with which persons with dormant schistosomiasis $(\eta_1 = 0)$ and virulent schistosomiasis ($\eta_2 = 0$) are tainted with TB, respectively, the BCG vaccine efficacy ($\epsilon_1 =$ 1), the therapeutic rate for TB-only affected persons ($\zeta_T = 0$), the decreased rate of contamination with schistosomiasis ($\psi = 0$), the modification parameter for comparative contagiousness of persons with aggressive TB and dormant schistosomiasis ($\Pi_1 = 0$), the therapeutic rate for TB for co-infected persons ($\zeta_{T1} = 0$), the rate of advancement from infectious TB/exposed to schistosomiasis to aggressive TB/aggressive schistosomiasis ($\sigma = 0$), and the advancement rate from unprotected from the two diseases (TB/schistosomiasis) to unprotected from TB/aggressive schistosomiasis ($\alpha_2 = 0$) without therapy for persons infected with TB and schistosomiasis, appropriately. The resultant effect is the eradication of the following human classes: persons externally re-tainted with TB ($I_{RT}=0$), persons who had undergone therapy for TB $(T_{HT}=0)$, persons who had undergone therapy for schistosomiasis $(T_{HS}=0)$, persons externally re-tainted with TB and unprotected against schistosomiasis $(I_{RS1} = 0)$, and persons externally re-tainted with TB/infectious schistosomiasis ($I_{RS2} = 0$). We arrive at the assertion:

Theorem 3.2. The DFE, \mathcal{E}_0 , of system (2.3) (or (3.2)) adjustment parameter for comparative contagiousness of humans re-tainted with TB ($\Theta_{RT}=0$), the therapeutic rate for schistosomiasis-only tainted persons ($\zeta_S=0$), the BCG vaccine waning ($\theta_V=0$), the impact of schistosomiasis on the BCG protection against TB ($\zeta_{TS}=0$), the comparative rates by which persons with dormant schistosomiasis ($\eta_1=0$) cum aggressive schistosomiasis ($\eta_2=0$) are tainted with TB, correspondingly, the therapeutic rate for TB-only tainted persons ($\zeta_T=0$), the depreciated rate of infection with schistosomiasis ($\psi=0$), the modification parameter for comparative contagiousness of persons with virulent TB and dormant schistosomiasis ($\Pi_1=0$), the therapeutic rate for TB for co-tainted persons ($\zeta_{T1}=0$), the rate of advancement from aggressive TB/unprotected against schistosomiasis to aggressive TB/aggressive schistosomiasis ($\sigma=0$), and the rate of advancement from unprotected against the two diseases (TB/schistosomiasis) to unprotected against TB/aggressive schistosomiasis ($\sigma=0$) and the BCG vaccine efficacy ($\sigma=0$) is globally asymptotically stable (GAS) assuming that $\mathcal{R}_{TS}^V < 1$ and unstable assuming

that $\mathcal{R}_{TS}^V > 1$.

Proof. To be able to demonstrate the GAS of the DFE, we use [29] theorem for comparison. To achieve this, we represent the tainted classes in (2.3) as

$$\frac{dX_2}{dt} = (F_o - V_o)X_2 - MX_2 \tag{3.16}$$

where

$$X_2 = [E_{HT}, I_{HT}, V_{TS}, E_{HS}, I_{HS}, E_{TS}, I_{ST}, E_{ST}, I_{TS}, I_S, L, J]^T$$
(3.17)

That is,

$$\begin{pmatrix} \dot{E}_{HT} \\ \dot{I}_{HT} \\ \dot{V}_{TS} \\ \dot{E}_{HS} \\ \dot{I}_{HS} \\ \dot{E}_{TS} \\ \dot{I}_{ST} \\ \dot{E}_{ST} \\ \dot{I}_{S} \\$$

$$F_o = \begin{pmatrix} F_{11(6\times6)} & F_{12(6\times6)} \\ F_{21(6\times6)} & F_{22(6\times6)} \end{pmatrix}, \tag{3.19}$$

$$V_o = \begin{pmatrix} V_{11(6\times6)} & V_{12(6\times6)} \\ V_{21(6\times6)} & V_{22(6\times6)} \end{pmatrix}, \tag{3.22}$$

where

with $Q_{1}^{'} = \kappa_{1} + \mu_{H}, Q_{2}^{'} = \delta_{T} + \mu_{H}, Q_{3}^{'} = \mu_{H}, Q_{4}^{'} = \alpha_{1} + \mu_{H}, Q_{5}^{'} = \delta_{S} + \mu_{H}, Q_{6}^{'} = \alpha_{2} + \kappa_{2} + \mu_{H}, Q_{7}^{'} = \sigma + \chi_{1}\delta_{T} + \mu_{H}, Q_{8}^{'} = \kappa_{3} + v_{1}\delta_{S} + \mu_{H}, Q_{9}^{'} = \chi_{2}\delta_{T} + v_{3}\delta_{S} + \mu_{H}, Q_{10}^{'} = \mu_{S}, Q_{11}^{'} = \mu_{L}, \text{ and } Q_{12}^{'} = \mu_{J}.$

We define the following coefficients as:

$$A_{1}^{'} = (1 - p)\omega, \quad B_{1}^{'} = \omega, \quad C_{1}^{'} = \frac{\Lambda_{H}(1 - \omega)}{J_{0}\mu_{H}}.$$
 (3.25)

The matrix M is defined as:

$$M = \begin{pmatrix} M_{11(6\times6)} & M_{12(6\times6)} \\ M_{21(6\times6)} & M_{22(6\times6)} \end{pmatrix}, \tag{3.26}$$

where

and

$$U_1 = 1 - (\frac{S_H + V_T}{N_H}), \quad U_2 = \frac{\Lambda_H}{J_0 \mu_H} - (\frac{S_H + V_T}{J_0 + \epsilon J}), \quad U_3 = \frac{\Lambda_S}{L_0 \mu_S} - \frac{S_S}{L_0 + \epsilon L}.$$
 (3.29)

which indicates that $M \geq 0$ already, $S_H + V_T \leq N_H \leq \Lambda_H/\mu_H$, $\frac{S_H + V_T}{J_0 + \epsilon J} \leq \frac{\Lambda_H}{J_0 \mu_H}$, and because $S_S \leq N_S \leq \Lambda_S/\mu_S$, $\frac{S_S}{L_0 + \epsilon L} \leq \frac{\Lambda_S}{L_0 \mu_S}$ for t > 0 in \mathcal{D}_V , it ensues that

$$\begin{pmatrix}
\dot{E}_{HT} \\
\dot{I}_{HT} \\
\dot{V}_{TS} \\
\dot{E}_{HS} \\
\dot{I}_{HS} \\
\dot{E}_{TS} \\
\dot{I}_{ST} \\
\dot{E}_{ST} \\
\dot{I}_{S} \\
\dot{L} \\
\dot{J}
\end{pmatrix}
\begin{pmatrix}
E_{HT} \\
I_{HT} \\
V_{TS} \\
E_{HS} \\
I_{HS} \\
E_{TS} \\
I_{ST} \\
E_{ST} \\
I_{TS} \\
I_{S} \\
L \\
J
\end{pmatrix},$$
(3.30)

Employing the authenticity that every eigenvalue belonging to the matrix $F_o - V_o$ possesses negative real components (review local stability result, while $\rho(F_oV_o^{-1}) < 1$ premised on $\mathcal{R}_{TS}^V < 1$ that is identical with $F_o - V_o$ possessing eigenvalues having negative real constituents while $\mathcal{R}_{TS}^V < 1$ [57], it therefore follows

3.4 Numerical simulation results

The system (2.3) is simulated, numerically, employing the values of parameters described in Table 4 and Table 5, respectively, to be able to consider the effect of changing some important or key parameters showing the impact of schistosomiasis on the immunogenicity of the BCG vaccine, the comparative contagiousness of externally re-tainted persons with TB, the comparative contagiousness of persons with dormant and virulent schistosomiasis, the proportion of unvaccinated persons, respectively, and vaccine waning of individuals vaccinated with BCG against TB on the population dynamics of the co-infection of TB-schistosomiasis.

Epidemiological and demographic parameters relevant to Nigeria are deployed in the numerical simulations performed in this section. Nigeria's overall population was estimated in 2017 as 189,559,502 [16,55]. Thus, it ensues that, at the disease-free equilibrium, the total population (Λ_H/μ_H) amounts to 189,559,502. The annual mean mortality rate for Nigeria (μ_H) is taken as 0.02041 [55]. Thus, the intermediate annual rate of recruitment of persons into the populace (Λ_H) amounts to 3,868,900. Additionally, the overall Nigerian incidence of TB was predicted as 407,000 [62] in 2017 whereas the whole incidence of schistosomiasis in Nigeria happened to have been nearly 29,000,000 [61]. Since it has already been established in the literature [4,37], that, the protective immunity induced by the BCG wanes from 10 to 15 years, it therefore implies that the parameter θ_V , which is indicative of the rate at which BCG vaccine-induced immunity wanes will adopt the values within [1/15, 1/10] which is [0.067, 0.1].

The aggregate incidence of TB at the point where the impact of schistosomiasis on BCG vaccine (ζ_{TS}) was fluctuated between 1 and 3 is depicted in Figure 1. It is obvious that the TB incidence increased most substantially as the impact of schistosomiasis on BCG protection against TB was elevated (i.e., $\zeta_{TS} \to 3$) on human individuals vaccinated with BCG and exposed to schistosomiasis; this is depicted in Figure 1(b). The simulated outcome implies that the incidence of TB in a populace could be elevated as the impact of schistosomiasis on BCG protection against TB increases. Reducing the impact of schistosomiasis on

Table 4: Parameter values (along with ranges) of the system (2.3)

Parameters	Values	Sample ranges	References
Farameters	varues	Sample ranges	neierences
	$0.02041 \text{ year}^{-1}$	[0.0143, 0.03]	[55]
μ_H		. , ,	
Λ_H	$3~868~900~{\rm year}^{-1}$	[3,000,000, 4,000,000]	[16]
eta_T	Variable year ^{−1}	[0, 2]	Assumed
ζ_{TS}	2.5 year^{-1}	[1, 3]	Assumed
ξ	$0.075 \mathrm{year}^{-1}$	[0, 1]	[24]
p	$0.1 \mathrm{year^{-1}}$	[0.05, 0.3]	[49]
f	$0.1~{\rm year^{-1}}$	[0, 0.005]	[49]
m	$0.1~\mathrm{year^{-1}}$	[0, 3]	[49]
π_1	$0.4~{\rm year^{-1}}$	[0, 1]	[24]
π_2	$0.45~\mathrm{year^{-1}}$	[0, 1]	[24]
π_3	$0.5~{ m year^{-1}}$	[0, 1]	[24]
k_1	$0.005 \ \mathrm{year^{-1}}$	[0.005, 0.05]	[9]
k_2	$0.005 \ \mathrm{year^{-1}}$	[0.005, 0.05]	[9]
k_3	$0.005 \ {\rm year^{-1}}$	[0.005, 0.05]	[9]
ζ_T	$0.75~\mathrm{year^{-1}}$	[0, 1]	Assumed
ζ_{T1}	$0.75~\mathrm{year^{-1}}$	[0.5, 1]	[41]
ζ_{T2}	$0.75~\mathrm{year^{-1}}$	[0.5, 1]	[41]
ζ_{T3}	$0.75~\mathrm{year^{-1}}$	[0.5, 1]	[41]
ζ_R	$0.75~\mathrm{year^{-1}}$	[0.5, 1]	[41]
ζ_{R1}	$0.75~\mathrm{year^{-1}}$	[0.5, 1]	[41]
ζ_S	$0.23~{\rm year^{-1}}$	[0.2, 0.5]	[27]
ζ_{S1}	$0.23~{ m year^{-1}}$	[0.2, 0.5]	[27]
ζ_{S2}	$0.23~{\rm year^{-1}}$	[0.2, 0.5]	[27]
ζ_{S3}	$0.23 \ {\rm year}^{-1}$	[0.2, 0.5]	[27]

BCG protection against TB (that is, $\zeta_{TS} \to 1$) as a method of control could lead to the prevention of nearly 18, 450, 000 cases of fresh TB contagions.

The aggregate incidence of TB where the comparative rate of contagiousness of externally re-tainted persons with TB (Θ_{RT}) was fluctuated between 0 to 1 as depicted in Figure 2. It was obvious that the incidence of TB rises as the comparative rate of contagiousness of externally re-tainted persons by TB elevates (that is, $\Theta_{RT} \rightarrow 1$) between persons vaccinated with BCG and unprotected against

Table 5: Parameter values (along with ranges) of the system (2.3) (cont'd)

Parameters	Values	Sample ranges	References
ω	$0.2~{\rm year^{-1}}$	[0, 1]	Assumed
$ heta_V$	$0.08~\mathrm{year^{-1}}$	[0.067, 0.1]	[4, 37]
ϵ_1	$0.9~{\rm year^{-1}}$	[0, 1]	Assumed
δ_T	$0.1~{ m year^{-1}}$	[0, 0.5]	[8]
δ_R	$0.1~{ m year^{-1}}$	[0, 0.5]	[8]
δ_S	$1.4~{ m year^{-1}}$	[0.365, 2.19]	[36]
α_1	$6.5~{ m year^{-1}}$	[0, 10]	[36]
$lpha_2$	$6.5~{ m year^{-1}}$	[0, 10]	[36]
α_3	$6.5~{ m year^{-1}}$	[0, 10]	[36]
ψ	$0.85~\mathrm{year^{-1}}$	[0.05, 0.85]	Assumed
σ	$0.5~{ m year^{-1}}$	[0, 1]	Assumed
χ_1	$0.65~\mathrm{year^{-1}}$	[0, 1]	Assumed
χ_2	$0.85~\mathrm{year^{-1}}$	[0, 1]	Assumed
η_1	$2.0 \ \mathrm{year^{-1}}$	[0, 3]	Assumed
η_2	$4.0~{\rm year^{-1}}$	[0, 5]	Assumed
Θ_{RT}	$0.5~{ m year^{-1}}$	[0, 1]	Assumed
Θ_{RS1}	$1.5~{ m year^{-1}}$	[0, 3]	Assumed
Θ_{RS2}	$1.5~{ m year^{-1}}$	[0, 3]	Assumed
Π_1	$1.8~{ m year^{-1}}$	[0, 3]	Assumed
Π_2	$2.0 \ \mathrm{year^{-1}}$	[0, 3]	Assumed
v_1	$0.001 \ {\rm year^{-1}}$	[0, 1]	Assumed
v_2	$0.002 \ {\rm year^{-1}}$	[0, 1]	Assumed
v_3	$0.003 \ {\rm year^{-1}}$	[0, 1]	Assumed
μ_S	$0.5 \mathrm{year^{-1}}$	[0, 1]	[27]
Λ_S	$73,000 \text{ year}^{-1}$	[73,000, 109,500]	[13]
ϵ	$182.5 \ { m year^{-1}}$	[0, 182.5]	[13]
eta_L	$1.475 \ { m year}^{-1}$	[0, 2]	Assumed
L_0	$10^8 \mathrm{year}^{-1}$	$[9 \times 10^7, 1 \times 10^8]$	[13]
N_e	$300 \mathrm{\ year^{-1}}$	[0, 800]	[13]
γ	$0.8468 \ \mathrm{year^{-1}}$	[0, 1]	[13]
μ_L	$328.5 \ { m year}^{-1}$	[100, 400]	[13]
eta_J	$4.19 \ {\rm year^{-1}}$	[0, 5]	Assumed
J_0	$9 \times 10^7 \text{ year}^{-1}$	$[8 \times 10^7, 9 \times 10^7]$	[13]
μ_J	$3.0 \mathrm{\ year^{-1}}$	[0, 3]	[13]
$ au_1$	0.1 year^{-1}	[0, 1]	Assumed
$ au_2$	$0.2~{\rm year^{-1}}$	[0, 1]	Assumed
ϕ	$500 \mathrm{year^{-1}}$	[0, 1,000]	[13]

schistosomiasis as revealed by the (b) part of Figure 2. The simulated outcome implies that the incidence of TB in a populace could be elevated just the same way that the comparative rate of contagiousness of externally re-tainted persons with TB elevates. Lowering the comparative rate of contagiousness of externally re-tainted persons with TB (that is, $\Theta_{RT} \to 0$) as a method of control may lead to the avoidance of nearly 9, 970, 000 cases of fresh TB contagions.

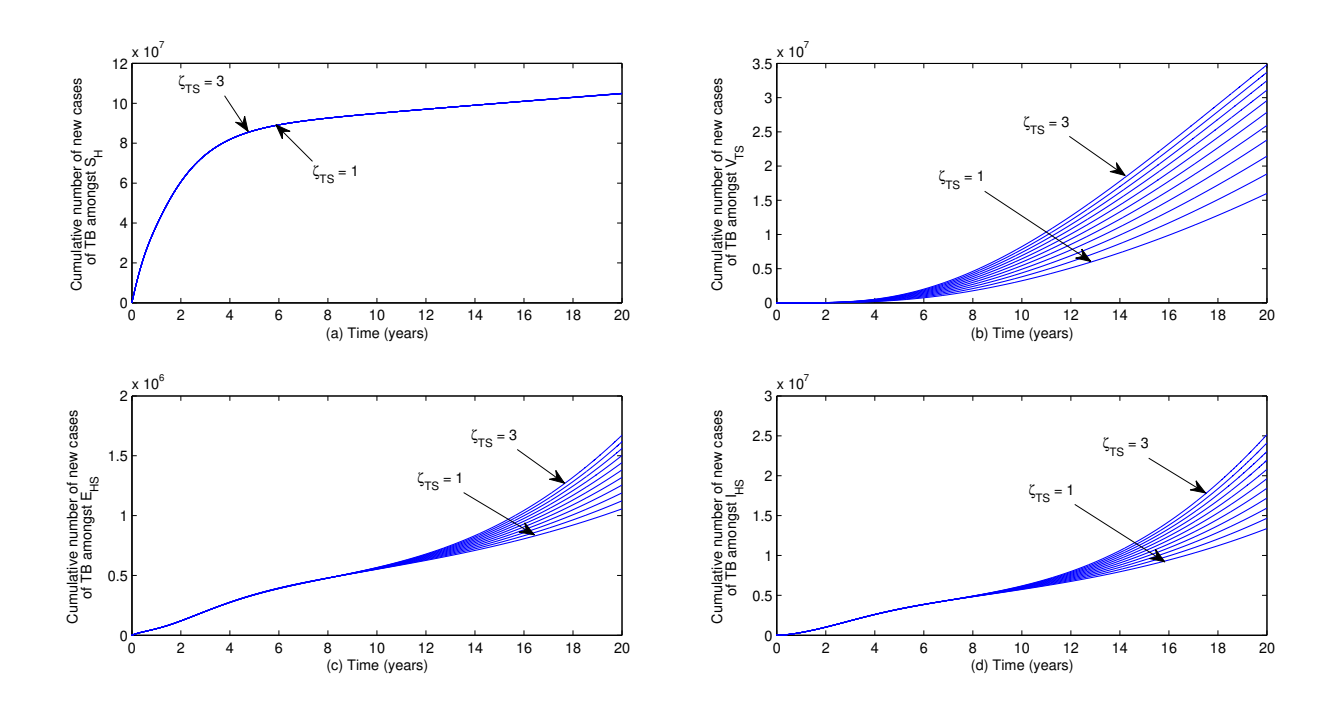


Figure 1: Aggregate number of fresh TB cases with $\beta_T = 1.5$, and fluctuated impact of schistosomiasis on BCG protection against TB (ζ_{TS}).

The aggregate incidence of TB at the point where the comparative contagiousness of persons with dormant schistosomiasis (η_1) was fluctuated between 0 to 3 is depicted in Figure 3. The simulated outcome implies that the incidence of TB was elevated as the comparative contagiousness of persons with dormant schistosomiasis elevates (that is, $\eta_1 \to 3$) between persons vaccinated with BCG and unprotected against schistosomiasis depicted in the (b) part of Figure 3. The simulated outcome implies that the incidence of TB in a populace could be elevated as the comparative contagiousness of persons with dormant schistosomiasis elevates. Lowering the comparative contagiousness of persons with dormant schistosomiasis (that is, $\eta_1 \to 0$) as a method of control could lead to the prevention of nearly 840, 000 cases of fresh TB contagions.

The aggregate incidence of TB at the point where the comparative contagiousness of persons with virulent schistosomiasis (η_2) was fluctuated between 0 to 5 is displayed in Figure 4. The simulated outcome depicts that the incidence of TB was elevated as the comparative contagiousness of persons with active schistosomiasis elevates (that is, $\eta_2 \to 5$) between persons vaccinated with BCG and unprotected against schistosomiasis revealed by the (b) part of Figure 4. The simulated outcome implies that the incidence of TB in a populace could be elevated as the comparative contagiousness of persons having virulent schistosomiasis elevates. Lowering the comparative contagiousness of persons with virulent schistosomiasis

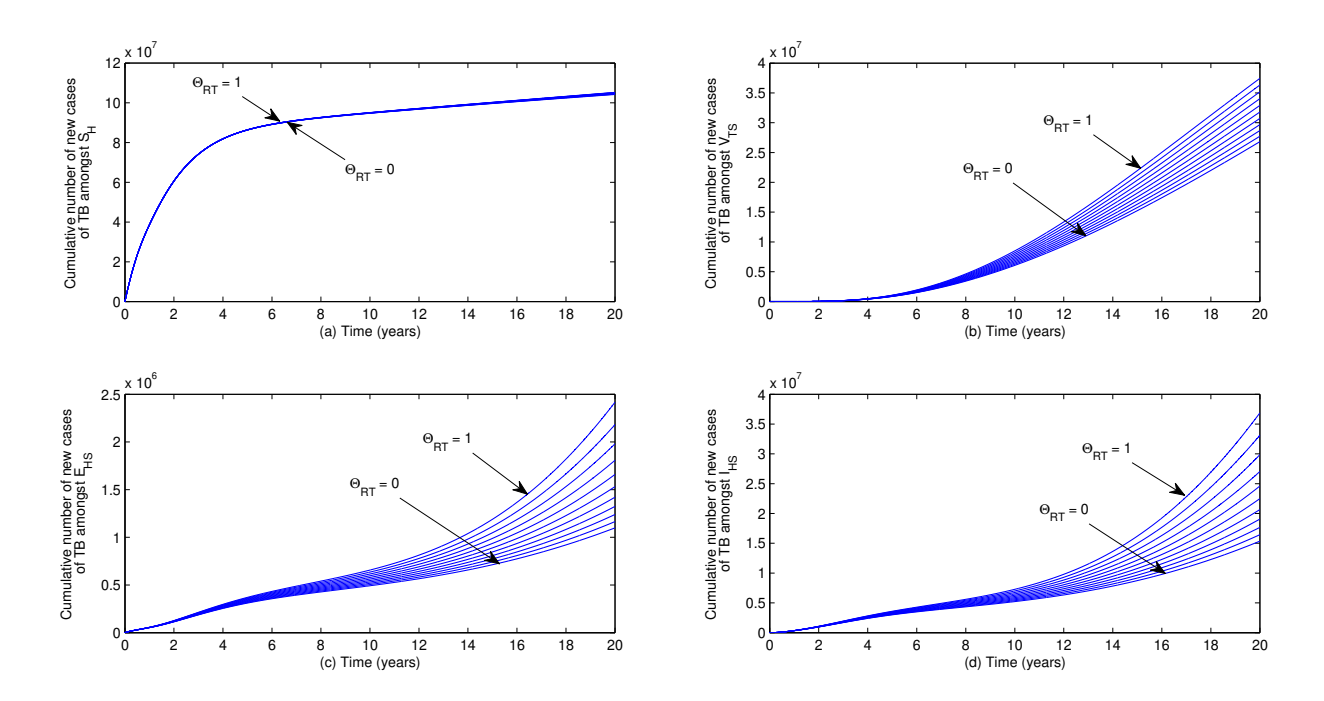


Figure 2: Aggregate number of fresh cases of TB at the point where $\beta_T = 1.5$, and fluctuated rate of comparative contagiousness of externally re-tainted persons with TB (Θ_{RT}).

(that is, $\eta_2 \to 0$) as a method of control could lead to the prevention of nearly 1, 200, 000 cases of fresh TB contagions.

The aggregate incidence of TB at the point where the proportion of persons unvaccinated with BCG (ω) was fluctuated between 0 to 1 is displayed in Figure 5. The simulated outcome implies that the incidence of TB was elevated as the proportion of persons unvaccinated with BCG elevates (that is, $\omega \to 1$) between persons vaccinated with BCG and unprotected against schistosomiasis as depicted by the (b) part of Figure 5. The simulated outcome that the incidence of TB in a populace could be elevated as the proportion of persons unvaccinated with BCG elevates. Lowering the proportion of persons unvaccinated with BCG (that is, $\omega \to 0$) as a strategy of control could lead to the prevention of about 33, 920, 000 cases of fresh TB contagions.

The aggregate incidence of TB at the point where the rate of vaccine waning of persons vaccinated with BCG against TB (θ_V) was fluctuated between 0.067 to 0.1 as depicted in Figure 6. The simulated outcome depicts that the incidence of TB was elevated as the rate of vaccine waning of persons vaccinated with BCG against TB elevates (that is, $\theta_V \to 0.1$) between persons vaccinated with BCG and exposed to schistosomiasis by the (b) part of Figure 6. The simulated outcome depicts that the incidence of TB in a populace could be increased as the rate of vaccine waning of persons vaccinated with BCG against

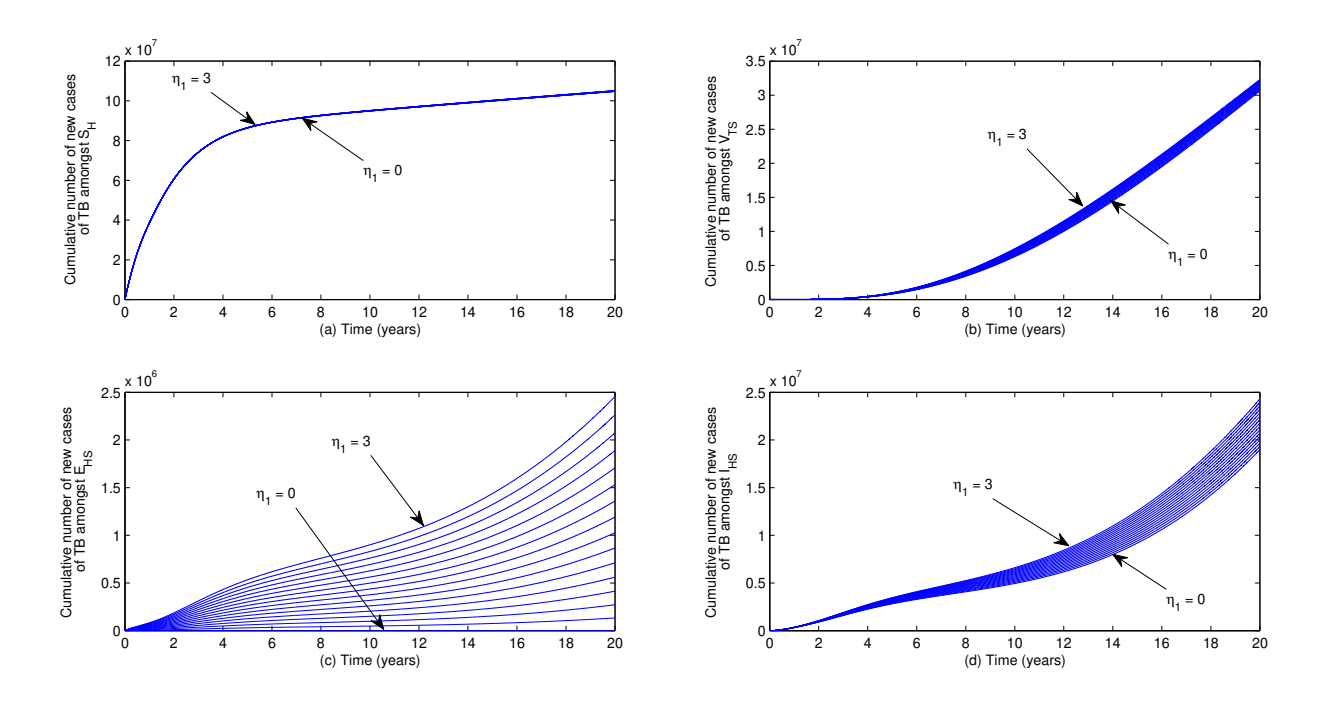


Figure 3: Aggregate number of fresh cases of TB at the point where $\beta_T = 1.5$, and fluctuated relative rate at which individuals with dormant schistosomiasis are tainted with TB (η_1) .

TB elevates. Lowering the rate of vaccine waning of persons vaccinated with BCG against TB (that is, $\theta_V \to 0.067$) as a strategy of control could lead to the prevention of about 950, 000 cases of fresh TB contagions.

4 Conclusion

In this study, we have created a novel mathematical model for studying how the impact of schistosomiasis infection on the immunogenicity of the BCG vaccine affects the use of vaccination as a measure of control against TB infection at population level. The infection-(disease-)free state of the model (2.3) was shown to be locally asymptotically stable (LAS) when the associated effective reproduction number was less than unity. In addition, model (2.3) was shown to exhibit the phenomenon of backward bifurcation initiated by the comparative contagiousness of humans re-tainted via TB, the therapeutic rate for schistosomiasis-only tainted persons, the BCG vaccine waning, the impact of schistosomiasis on the BCG protection against TB, the BCG vaccine waning, the comparative rates via which persons having dormant schistosomiasis cum contagious schistosomiasis are tainted with TB, respectively, the BCG vaccine efficacy, the treatment rate for TB, the decreased infection rate with schistosomiasis, the adjustment parameter for comparative

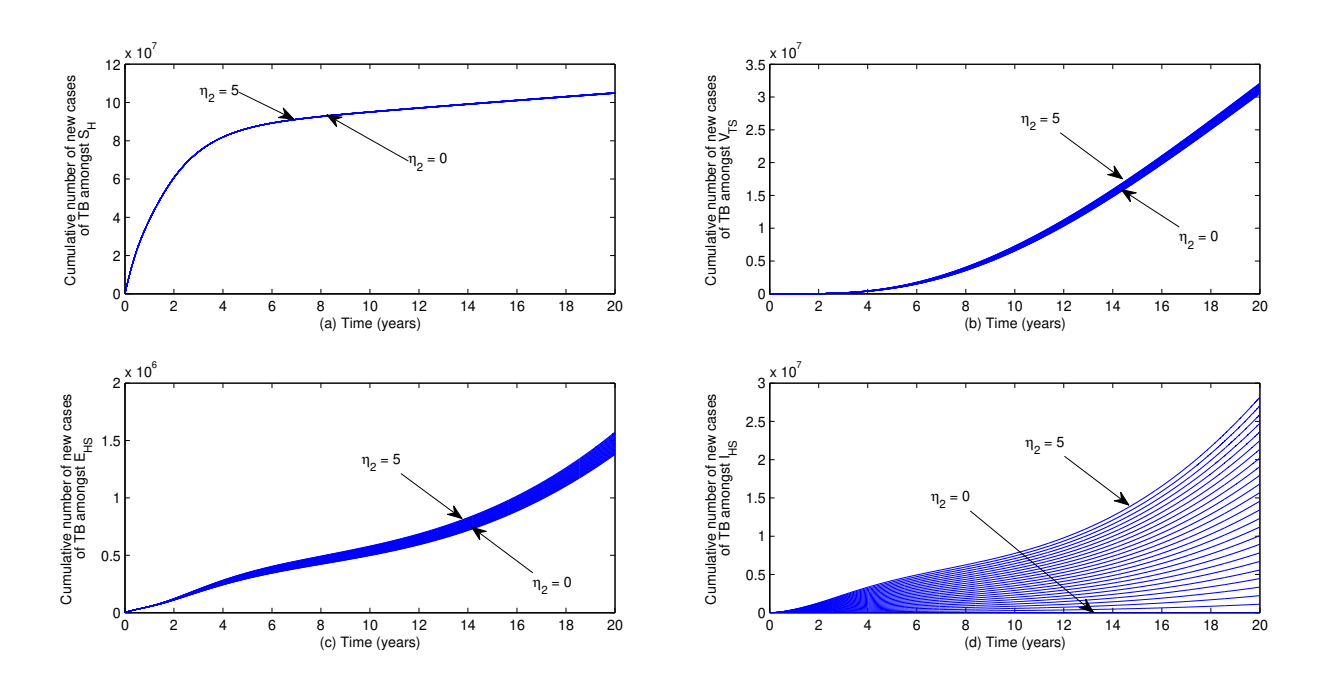


Figure 4: Aggregate number of fresh cases of TB at the point where $\beta_T = 1.5$, and fluctuated comparative rate at which persons with virulent schistosomiasis are tainted with TB (η_2) .

contagiousness of persons with contagious TB and dormant schistosomiasis, the therapeutic rate for TB for co-infected persons, the transition rate from contagious TB/unprotected against schistosomiasis to contagious TB/contagious schistosomiasis, and the rate of transition from unprotected against to the two epidemics (TB/schistosomiasis) to unprotected against TB/contagious schistosomiasis. In addition, a unique case of the model (2.3) was revealed to be globally asymptotically stable (GAS), when the connected effective reproduction number was less than unity.

Results numerically simulated from the model system (2.3) revealed that a reduction in the significance of key parameters like the comparative rate of contagiousness of externally re-tainted persons with TB, the rate of comparative contagiousness of persons with dormant and contagious schistosomiasis, respectively, the impact of schistosomiasis on the BCG vaccine and the proportion of persons unvaccinated with BCG vaccine could lead to a significant decrease in the prevalence of TB-schistosomiasis co-infection in the populace.

It has been revealed via this study that control programmes for TB and schistosomiasis which support the corresponding therapy for contagious cases of the two epidemics, vaccination of susceptible humans with the BCG vaccine (with high vaccine efficacy and low vaccine waning) against TB contamination and the intentional reduction of unvaccinated persons who are susceptible to TB must be rigorously

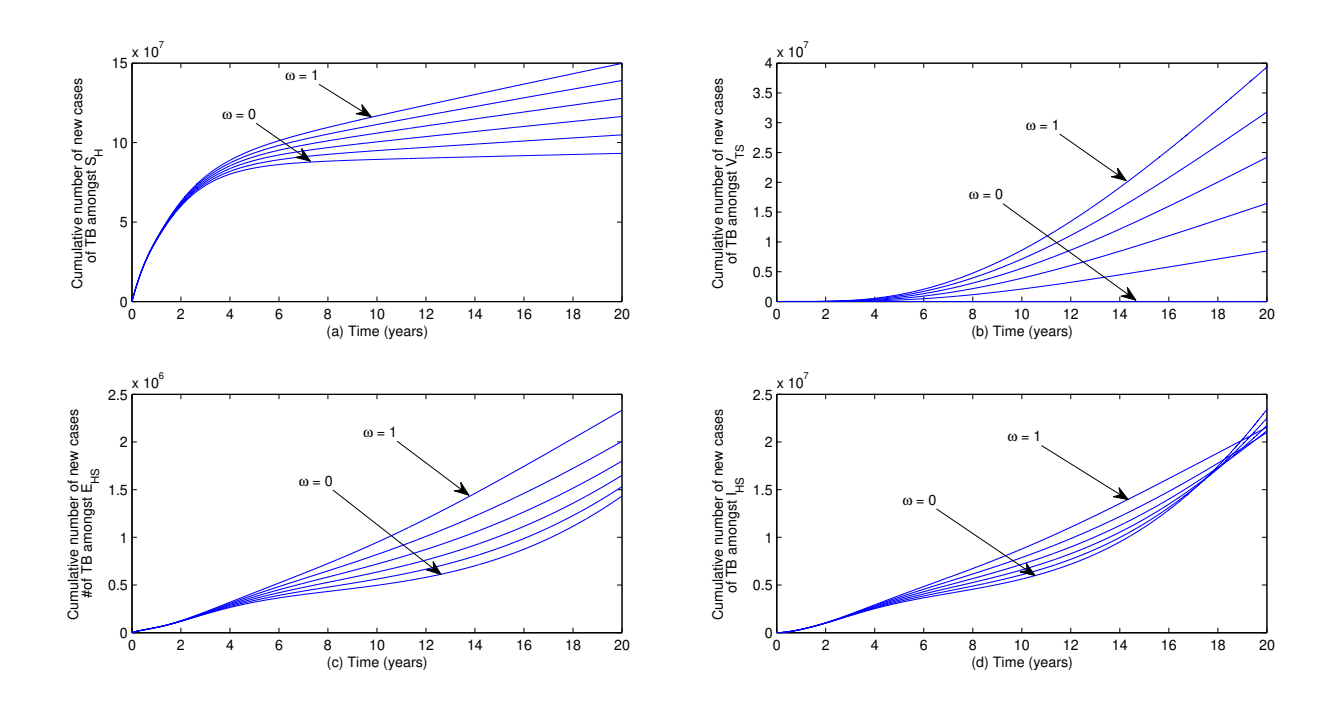


Figure 5: Aggregate number of fresh cases of TB at the point where $\beta_T = 1.5$, and fluctuated proportion of persons unvaccinated with BCG against TB (ω).

chased, considering that programmes such as these could lead to substantial decrease in the weight of the co-infection of TB-schistosomiasis in the population. Furthermore, to stop any opportunity that would promote the occurrence of the backward bifurcation phenomenon, measures of control should be focused on the parameters that provoke it, namely: the comparative contagiousness of humans re-tainted with TB (Θ_{RT}), the treatment rate for schistosomiasis-only infected persons (ζ_S), the BCG vaccine waning (θ_V), the impact of schistosomiasis on the BCG protection against TB (ζ_{TS}), the comparative rates via which persons having dormant schistosomiasis (η_1) cum contagious schistosomiasis (η_2) are tainted with TB, correspondingly, the BCG vaccine efficacy (ϵ_1), the treatment rate for TB (ζ_T), the depreciated rate of contamination with schistosomiasis (ψ), the modification parameter for comparative contagiousness of persons with virulent TB and dormant schistosomiasis (Π_1), the treatment rate for TB for co-infected persons (ζ_{T1}), the rate of transition from contagious TB/unprotected against schistosomiasis to contagious TB/contagious schistosomiasis (σ), and the transition rate from unprotected against the two diseases (TB/schistosomiasis) to unprotected against TB/contagious schistosomiasis (σ_2).

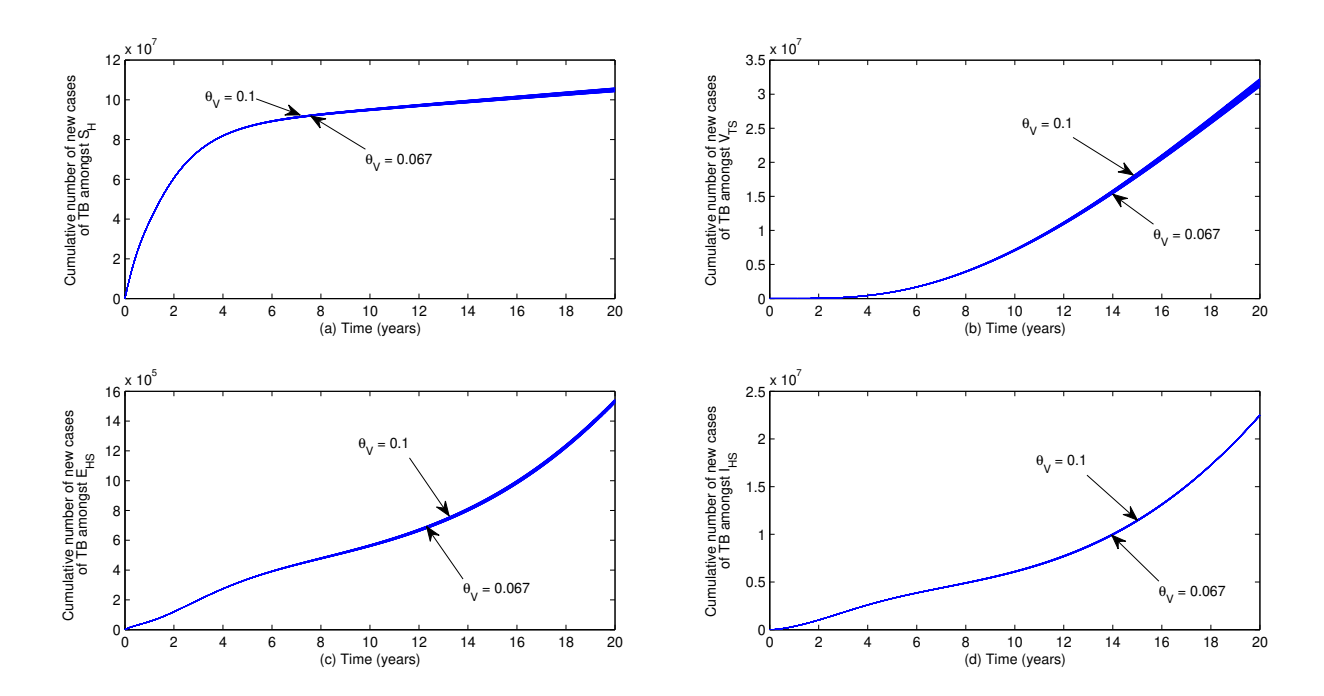


Figure 6: Aggregate number of fresh cases of TB at the point where $\beta_T = 1.5$, and fluctuated rate of vaccine waning of persons vaccinated with BCG against TB (θ_V).

References

- [1] Ako, I. I. (2024). Uncertainty and sensitivity analysis of the effective reproduction number for a deterministic mathematical model for tuberculosis-schistosomiasis co-infection dynamics. *Transactions of the Nigerian Association of Mathematical Physics*, 20, 45–60.
- [2] Ako, I. I., Akhaze, R. U., & Olowu, O. O. (2021). The impact of reduced re-infection on schistosomiasis transmission dynamics: a theoretical study. *Journal of Nigerian Association of Mathematical Physics*, 59, 61–74.
- [3] Ako, I. I., & Olowu, O. O. (2024). Causes of backward bifurcation in a tuberculosis-schistosomiasis co-infection dynamics. *Earthline Journal of Mathematical Sciences*, 14(4), 655–695. https://doi.org/10.34198/ejms.14424.655695
- [4] Anderson, E. J., Webb, E. L., Mawa, P. A., Kizza, M., Lyadda, N., Nampijja, M., & Elliot, A. M. (2012). The influence of BCG vaccine strain on mycobacteria-specific and non-specific immune responses in a prospective cohort of infants in Uganda. *Vaccine*, 30, 2083–2089. https://doi.org/10.1016/j.vaccine.2012.01.053
- [5] Athithan, S., & Ghosh, M. (2013). Mathematical modelling of TB with the effects of case detection and treatment. *International Journal of Dynamics and Control*, 1, 223–230.

- [6] Barbour, A. D. (1982). Schistosomiasis. In R. M. Anderson (Ed.), *Population Dynamics of Infectious Diseases* (pp. 180–208). Chapman and Hall, London. https://doi.org/10.1007/978-1-4899-2901-3_6
- [7] Bhunu, C. P. (2011). Mathematical analysis of a three-strain tuberculosis transmission model. *Applied Mathematical Modelling*, 35, 4647-4660. https://doi.org/10.1016/j.apm.2011.03.037
- [8] Bhunu, C. P., Garira, W., & Magombedze, G. (2009). Mathematical analysis of a two-strain HIV/AIDS model with antiretroviral treatment. *Acta Biotheoretica*, 57(3), 361–381. https://doi.org/10.1007/s10441-009-9080-2
- [9] Blower, S. M., McLean, A. R., Porco, T. C., Small, P. M., Hopewell, P. C., Sanchez, M. A., & Moss, A. R. (1995). The intrinsic transmission dynamics of tuberculosis epidemics. *Nature Medicine*, 1, 815–821. https://doi.org/10.1038/nm0895-815
- [10] Castillo-Chavez, C., & Song, B. (2004). Dynamical models of tuberculosis and their applications. *Mathematical Biosciences and Engineering*, 1(2), 361–404. https://doi.org/10.3934/mbe.2004.1.361
- [11] Chen, Z., Zou, L., Shen, D., Zhang, W., & Ruan, S. (2010). Mathematical modelling and control of schistosomiasis in Hubei Province, China. *Acta Tropica*, 115, 119–125. https://doi.org/10.1016/j.actatropica.2010.02.012
- [12] Chitsulo, L., Engels, D., Montresor, A., & Savioli, L. (2000). The global status of schistosomiasis and its control. Acta Tropica, 77, 41–51. https://doi.org/10.1016/S0001-706X(00)00122-4
- [13] Chiyaka, E., & Garira, W. (2009). Mathematical analysis of the transmission dynamics of schistosomiasis in the human-snail hosts. *Journal of Biological Systems*, 17, 397–423. https://doi.org/10.1142/S0218339009002910
- [14] Chiyaka, E. T., Magombedze, G., & Mutimbu, L. (2010). Modelling within-host parasite dynamics of schistosomiasis. Computational and Mathematical Methods in Medicine, 11(3), 255–280. https://doi.org/ 10.1080/17486701003614336
- [15] Cohen, J. E. (1977). Mathematical models of schistosomiasis. *Annual Review of Ecology and Systematics*, 8, 209–233. https://doi.org/10.1146/annurev.es.08.110177.001233
- [16] Countrymeters. (2017). Nigeria Population. Retrieved from https://countrymeters.info/en/Nigeria (Accessed on July 19, 2018).
- [17] Desaleng, D., & Koya, P. R. (2016). Modeling and analysis of multi-drug-resistant tuberculosis in densely populated areas. American Journal of Applied Mathematics, 4(1), 1–10. https://doi.org/10.11648/j.ajam. 20160401.11
- [18] Diaby, M. A., Iggidr, A., Sy, M., & Sene, A. (2014). Global analysis of a schistosomiasis infection model with biological control. *Applied Mathematics and Computation*, 246, 731–742. https://doi.org/10.1016/j.amc. 2014.08.061

- [19] Elias, D., Wolday, D., Akuffo, H., Petros, B., Bronner, U., & Britton, S. (2001). Effect of deworming on human T cell responses to mycobacterial antigens in helminth-exposed individuals before and after Bacille Calmette-Guérin (BCG) vaccination. Clinical and Experimental Immunology, 123(2), 219–225. https://doi. org/10.1046/j.1365-2249.2001.01446.x
- [20] Elias, D., Akuffo, H., Thors, C., Pawlowski, A., & Britton, S. (2005a). Low-dose chronic *Schistosoma mansoni* infection increases susceptibility to *Mycobacterium bovis* BCG infection in mice. *Clinical and Experimental Immunology*, 139(3), 398-404. https://doi.org/10.1111/j.1365-2249.2004.02719.x
- [21] Elias, D., Akuffo, H., Pawlowski, A., Haile, M., Schön, T., & Britton, S. (2005b). Schistosoma mansoni infection reduces the protective efficacy of BCG vaccination against virulent Mycobacterium tuberculosis. Vaccine, 23(11), 1326-1334. https://doi.org/10.1016/j.vaccine.2004.09.038
- [22] Elias, D., Akuffo, H., & Britton, S. (2006). Helminths could influence the outcome of vaccines against TB in the tropics. *Parasite Immunology*, 28(10), 507–513. https://doi.org/10.1111/j.1365-3024.2006.00854.x
- [23] Elias, D., Britton, S., Aseffa, A., Engers, H., & Akuffo, H. (2008). Poor immunogenicity of BCG in a helminth-infected population is associated with increased *in vitro* TGF-β production. *Vaccine*, 26(31), 3897–3902. https://doi.org/10.1016/j.vaccine.2008.04.083
- [24] Feng, Z., Castillo-Chavez, C., & Capurro, A. F. (2000). A model for tuberculosis with exogenous reinfection. Theoretical Population Biology, 57, 235–247. https://doi.org/10.1006/tpbi.2000.1451
- [25] Feng, Z., Curtis, J., & Minchella, D. J. (2001). The influence of drug treatment on the maintenance of schistosome genetic diversity. *Journal of Mathematical Biology*, 43, 52-68. https://doi.org/10.1007/ s002850100092
- [26] Feng, Z., Li, C.-C., & Milner, F. A. (2002). Schistosomiasis models with density dependence and age of infection in snail dynamics. *Mathematical Biosciences*, 177-178, 271–286. https://doi.org/10.1016/S0025-5564(01) 00115-8
- [27] Feng, Z., Eppert, A., Milner, F. A., & Minchella, D. J. (2004). Estimation of parameters governing the transmission dynamics of schistosomes. *Applied Mathematics Letters*, 17, 1105–1112. https://doi.org/10.1016/j.aml.2004.02.002
- [28] Inobaya, M. T., Olveda, R. M., Chau, T. N. P., Olveda, D. U., & Ross, A. G. P. (2014). Prevention and control of schistosomiasis: A current perspective. Research Reports in Tropical Medicine, 5, 65-75. https://doi.org/10.2147/RRTM.S44274
- [29] Lakshmikantham, V., Leela, S., & Martynyuk, A. A. (1991). Stability analysis of nonlinear systems. SIAM Review, 33(1), 152–154. https://doi.org/10.1137/1033038
- [30] Li, X. X., & Zhou, X. N. (2013). Coinfection of tuberculosis and parasitic diseases in humans: A systematic review. *Parasites & Vectors*, 6, 79. https://doi.org/10.1186/1756-3305-6-79

- [31] Macdonald, G. (1965). The dynamics of helminth infections with special reference to schistosomes. Transactions of the Royal Society of Tropical Medicine and Hygiene, 59(5), 489–506. https://doi.org/10.1016/0035-9203(65)90152-5
- [32] Milner, F. A., & Zhao, R. (2008). A deterministic model of schistosomiasis with spatial structure. *Mathematical Biosciences and Engineering*, 5(3), 505–522. https://doi.org/10.3934/mbe.2008.5.505
- [33] Monin, L., Griffiths, K. L., Lam, W. Y., Gopal, R., Kang, D. D., Ahmed, M., Rajamanickam, A., Cruz-Lagunas, A., Zúñiga, J., Babu, S., Kolls, J. K., Mitreva, M., Rosa, B. A., Ramos-Payan, R., Morrison, T. E., Murray, P. J., Rangel-Moreno, J., Pearce, E. J., & Khader, S. A. (2015). Helminth-induced arginase-1 exacerbates lung inflammation and disease severity in tuberculosis. *The Journal of Clinical Investigation*, 125(12), 4699–4713. https://doi.org/10.1172/JCI77378
- [34] Moualeu, D. P., Weiser, M., Ehrig, R., et al. (2015). Optimal control for a tuberculosis model with undetected cases in Cameroon. *Communications in Nonlinear Science and Numerical Simulation*, 20, 986–1003. https://doi.org/10.1016/j.cnsns.2014.06.037
- [35] Mushayabasa, S., & Bhunu, C. P. (2011). Modelling schistosomiasis and HIV/AIDS codynamics. Computational and Mathematical Methods in Medicine, 2011, Article ID 846174. https://doi.org/10.1155/2011/846174
- [36] Ngarakana-Gwasira, E. T., Bhunu, C. P., Masocha, M., & Mashonjowa, E. (2016). Transmission dynamics of schistosomiasis in Zimbabwe: A mathematical and GIS approach. *Communications in Nonlinear Science and Numerical Simulation*, 35, 137–147. https://doi.org/10.1016/j.cnsns.2015.11.005
- [37] Nguipdop-Djomo, P., Heldal, E., Rodrigues, L. C., Abubakar, I., & Mangtani, P. (2015). Duration of BCG protection against tuberculosis and change in effectiveness with time since vaccination in Norway: A retrospective population-based cohort study. *The Lancet Infectious Diseases*, 16(2), 219–226. https://doi.org/10.1016/S1473-3099(15)00400-4
- [38] Okosun, K. O., & Smith?, R. (2017). Optimal control analysis of malaria-schistosomiasis co-infection dynamics. Mathematical Biosciences and Engineering, 14(2), 377–405. https://doi.org/10.3934/mbe.2017024
- [39] Okuonghae, D. (2013). A mathematical model of tuberculosis transmission with heterogeneity in disease susceptibility and progression under a treatment regime for infectious cases. *Applied Mathematical Modelling*, 37, 6786–6808. https://doi.org/10.1016/j.apm.2013.01.039
- [40] Okuonghae, D. (2014). Lyapunov functions and global properties of some tuberculosis models. *Journal of Applied Mathematics and Computation*. https://doi.org/10.1007/s12190-014-0811-4
- [41] Okuonghae, D., & Aihie, V. (2008). Case detection and direct observation therapy strategy (DOTS) in Nigeria: Its effect on TB dynamics. *Journal of Biological Systems*, 16(1), 1–31. https://doi.org/10.1142/S0218339008002344
- [42] Okuonghae, D., & Aihie, V. U. (2010). Optimal control measures for tuberculosis mathematical models including immigration and isolation of infective cases. *Journal of Biological Systems*, 18(1), 17–54. https://doi.org/10.1142/s0218339010003160

- [43] Okuonghae, D., & Ikhimwin, B. O. (2016). Dynamics of a mathematical model for tuberculosis with variability in susceptibility and disease progressions due to difference in awareness level. Frontiers in Microbiology, 6, 1530. https://doi.org/10.3389/fmicb.2015.01530
- [44] Okuonghae, D., & Korobeinikov, A. (2007). Dynamics of tuberculosis: The effect of direct observation therapy strategy (DOTS) in Nigeria. *Mathematical Modelling of Natural Phenomena*, 2(1), 101–113. https://doi.org/10.1051/mmnp:2008013
- [45] Okuonghae, D., & Omosigho, S. E. (2011). Analysis of a mathematical model for tuberculosis: What could be done to increase case detection? *Journal of Theoretical Biology*, 269, 31–45. https://doi.org/10.1016/j.jtbi.2010.09.044
- [46] Olowu, O., & Ako, I. (2023). Computational investigation of the impact of availability and efficacy of control on the transmission dynamics of schistosomiasis. *International Journal of Mathematical Trends and Technology*, 69(8), 1–9. https://doi.org/10.14445/22315373/IJMTT-V69I8P501
- [47] Olowu, O., Ako, I. I., & Akhaze, R. I. (2021). Theoretical study of a two-patch metapopulation schistosomiasis model. Transactions of the Nigerian Association of Mathematical Physics, 14, 53–68.
- [48] Olowu, O., Ako, I. I., & Akhaze, R. I. (2021). On the analysis of a two-patch schistosomiasis model. Transactions of the Nigerian Association of Mathematical Physics, 14, 69–78.
- [49] Porco, T. C., & Blower, S. M. (1998). Quantifying the intrinsic transmission dynamics of tuberculosis. https://doi.org/10.1006/tpbi.1998.1366
- [50] Potian, J. A., Rafi, W., Bhatt, K., McBride, A., Gause, W. C., & Salgame, P. (2011). Preexisting helminth infection induces inhibition of innate pulmonary anti-tuberculosis defense by engaging the IL-4 receptor pathway. *Journal of Experimental Medicine*, 208(9), 1863–1874. https://doi.org/10.1084/jem.20091473
- [51] Qi, L., & Cui, J. (2013). A schistosomiasis model with mating structure. Abstract and Applied Analysis, 2013, Article ID 741386, 9 pages. https://doi.org/10.1155/2013/741386
- [52] Qi, L., Xue, M., Cui, J., Wang, Q., & Wang, T. (2018). Schistosomiasis model and its control in Anhui Province. Bulletin of Mathematical Biology, 80, 2435–2451. http://doi.org/10.1007/s11538-018-0474-7
- [53] Salgame, P., Yap, G. S., & Gause, W. C. (2013). Effect of helminth-induced immunity on infections with microbial pathogens. *Nature Immunology*, 14(11), 1118–1126. https://doi.org/10.1038/ni.2736
- [54] Sharomi, O. Y., Safi, M. A., Gumel, A. B., & Gerberry, D. J. (2017). Exogenous re-infection does not always cause backward bifurcation in TB dynamics. *Applied Mathematics and Computation*, 298, 322–335. https://doi.org/10.1016/j.amc.2016.11.009
- [55] UNAIDS-WHO. (2004). Epidemiological Fact Sheet. Retrieved from http://www.unaids.org.
- [56] United Nations. (2016). Sustainable Development Goals. Retrieved from https://sustainabledevelopment.un.org/topics/sustainabledevelopmentgoals (accessed 27 July, 2016).

- [57] van den Driessche, P., & Watmough, J. (2002). Reproduction numbers and sub-threshold endemic equilibria for compartmental models of disease transmission. *Mathematical Biosciences*, 180, 29–48. https://doi.org/ 10.1016/S0025-5564(02)00108-6
- [58] Waaler, H., Geser, A., & Andersen, S. (1962). The use of mathematical models in the study of the epidemiology of tuberculosis. *American Journal of Public Health and the Nations Health*, 52(6), 1002–1013. https://doi.org/10.2105/AJPH.52.6.1002
- [59] World Health Organization (WHO). (2008). Global Tuberculosis Control-Surveillance.
- [60] World Health Organization (WHO). (2015). Global Tuberculosis Report. WHO Press, Geneva, Switzerland.
- [61] World Health Organization (WHO). (2017). Schistosomiasis Factsheet 2017. WHO Press, Geneva, Switzerland.
- [62] World Health Organization (WHO). (2018a). Tuberculosis Factsheet 2018. WHO Press, Geneva, Switzerland.
- [63] World Health Organization (WHO). (2018b). Global Tuberculosis Report 2018. WHO Press, Geneva, Switzerland.
- [64] World Health Organization (WHO). (2023). Global Tuberculosis Report 2023. WHO Press, Geneva, Switzerland.
- [65] World Health Organization (WHO). (2023). Schistosomiasis Factsheet 2023. WHO Press, Geneva, Switzerland.
- [66] World Health Organization (WHO). (2024). Tuberculosis Factsheet 2024. WHO Press, Geneva, Switzerland.
- [67] Woolhouse, M. E. J. (1991). On the application of mathematical models of schistosome transmission dynamics I: natural transmission. *Acta Tropica*, 49, 241. https://doi.org/10.1016/0001-706X(91)90077-W
- [68] Zhao, R. & Milner, F. A. (2008). A mathematical model of *Schistosoma mansoni* in *Biomphalaria glabrata* with control strategies. *Bulletin of Mathematical Biology*, 70(7), 1886-1905. https://doi.org/10.1007/s11538-008-9330-5
- [69] Zou, L. & Ruan, S. (2015). Schistosomiasis transmission and control in China. *Acta Tropica*, 143, 51-57. https://doi.org/10.1016/j.actatropica.2014.12.004

This is an open access article distributed under the terms of the Creative Commons Attribution License (http://creativecommons.org/licenses/by/4.0/), which permits unrestricted, use, distribution and reproduction in any medium, or format for any purpose, even commercially provided the work is properly cited.